P.W. LÈVY, J.M. LOMAN, K.J. SWYLER and R.W. KLAFFKY, 1981: *"Radiation Damage Studies on Synthetic NaCl Crystals and Natural Rock Salt for Radioactive Waste Disposal Applications"*, in "The Technology of High–Level Nuclear Waste Disposal", Vol. 1, (DOE/TIC–4621), ed. P.L. Hoffmann, (Tech. Info. Ctr., U.S. Dept. of Energy, Oak Ridge, TN), p. 136–167.

P.W. LEVY, J.M. LOMAN and J.A. KIERSTEAD, 1984: *"Radiation Induced F–center and Colloid Formation in Synthetic NaCl and Natural Rock Salt: Applications to Radioactive Waste Repositories"*, Nuc. Instr. Meth. Phys. Res. **B1**, 549–556.

A.B. LIDIARD, 1979: *"Energy Stored in Irradiated NaCl"*, Phil. Mag. **A39**, 647–659.

J.M. LOMAN, P.W. LEVY and K.J. SWYLER, 1982: *"Radiation Induced Sodium Metal Colloid Formation in Natural Rock Salt from Different Geological Localities"*, in "Scientific Basis for Nuclear Waste Management", Vol. 6, Ed. S.V. Topp, (Elsevier, New York), p. 433–440.

G. VAN OPBROEK and H.W. DEN HARTOG, 1985: *"Radiation Damage of NaCl: Dose Rate Effects"*, J. Phys. C: Solid State Phys. **18**, 257–268.

W.J. SOPPE, 1993: *"Computer Simulation of Radiation Damage in NaCl by using a Kinetic Rate Reaction Model"*, J. Phys.: Condensed Matter **5**, 3519–3540.

W.J. SOPPE and J. PRIJ, 1994: *"Radiation Damage in a Rock Salt Nuclear Waste Repository"*, Nuc. Techn. **107**, 243–253.

W.J. SOPPE, H. DONKER, A. GARCIA CELMA and J. PRIJ, 1994: *"Radiation Induced Stored Energy in Rock Salt"*, J. Nuc. Mat. **217**, 1–31.

C.J. SPIERS, J.L. URAI, G.S. LISTER, J.N. BOLAND and H.J. ZWART, 1986: *"The Influence of Fluid–Rock Interaction on the Rheology of Salt Rock"*, Nuclear Science and Technology Series, EUR–10399, Commission of the European Communities, Luxembourg, 131 p.

K.J. SWYLER, R.W. KLAFFKY and P.W. LEVY, 1979: *"Radiation Damage Studies on Natural and Synthetic Rock Salt for Waste disposal Applications"*, in "Scientific Basis for Nuclear Waste Management", Vol. 1, Ed. G.J. McCarthy (Plenum, New York), p. 349–354.

K.J. SWYLER, R.W. KLAFFKY and P.W. LEVY, 1980: *"Recent Studies on Radiation Damage Formation in Synthetic NaCl and Natural Rock Salt for Radioactive Waste Disposal Applications"*, in "Scientific Basis for Nuclear Waste Management", Vol. 2, Ed. C.J.M. Northrup Jr.,(Plenum, New York), p. 553–560.

ON THE RELATIONSHIP BETWEEN STORED ENERGY AND COLLOIDAL SODIUM PRODUCTION IN IRRADIATED ROCK SALT

H. Donker, W.J. Soppe and A. García Celma

ABSTRACT

A few parameters of the theoretical models used to describe the formation of radiation damage in rock salt were critically reviewed. It is discussed that the back reaction used in the models should be described as $\gamma = 10^{16} \exp(-0.4/kT)$ and that for the conversion factor between defect concentrations and stored energy a value of 5 eV/F–H pair should be used. With these modified parameters the models were compared with the experimental results of Jenks and Bopp and the experimental results obtained from the GIF A irradiation experiments.

1. INTRODUCTION

The first model describing the formation of radiation damage in alkali halides was developed by Jain and Lidiard [1977]. This model was later modified by Van Opbroek and den Hartog [1985], according to a proposal of Lidiard [1979]. This modification, the inclusion of a back reaction, was introduced in order to be able to explain the experimental results of Jenks and Bopp [1974;1977] and Jenks et al. [1975].

A disadvantage of this model is that it does not describe the nucleation stage of the colloids and dislocation loops. Moreover, the effects of impurities, strain and grain boundaries are not taken into account. Recently two new, slightly different models based on the old Jain–Lidiard model, but with extensions describing the nucleation stage have been developed [Soppe, 1993; Seinen et al.,1992].

In a recent paper [Soppe et al., 1994] the experimental results on radiation damage

formation in NaCl and the theoretical models used to describe this process were reviewed. Since then the availability of new experimental evidence and a thorough study of the literature has convinced us that a few parameters used in the models have to be modified. These modifications will be discussed below. A comparison with computer simulations made with the modified Jain–Lidiard model [Opbroek and den Hartog, 1985] and the model of Soppe [1993] using these modified parameters with the experimental results of Jenks and Bopp [1974; 1977] and Jenks et al. [1975] and our experimental data obtained for heavily irradiated Asse speisesalz samples [Donker and Garcia Celma, 1995] will be made.

2.   THE BACK REACTION

In the modified Jain–Lidiard model [van Opbroek and den Hartog, 1985] as well as in the model of Soppe [1993] the probability for the back reaction between the F–centres and the Cl$_2$ molecules is described by:

$$\gamma = \gamma_0 \exp\left(\frac{-E_\gamma}{kT}\right) \tag{1}$$

The assumed values for the pre–exponential factor γ_0 used in these models are 3×10^{18} and 10^{18} cm^{-2} respectively, and for the activation energy E_γ values of 0.6 and 0.55 eV were used.

Reasons can be given that the values used in both models for the pre–exponential factor are two orders of magnitude to high. γ_0 should be of the order of 10^{16} cm^{-2} which is a normal value for reactions between point defects [Seinen, private communication].

The values used for the activation energy E_γ are not known with great accuracy. Soppe obtained 0.55 eV from fitting his model to the experimental data of Jenks and Bopp, while Lidiard based the 0.6 eV on the annealing experiments of these authors, who derived an overall activation energy E_a of 1.7 eV for the back reaction. Seinen [1994], however, has measured the activation energy of the back reaction on doped samples and reported values for this energy of 1.2, 1.5 and 1.7 eV depending on the method. Since the origin of the difference between the various measurements is not yet clear, we will use their average value i.e. 1.5 eV.

In the models, the back reaction is assumed to proceed via evaporation of F–centres from the colloids which then diffuse to and recombine with the molecular Cl$_2$ centres. This last, recombination step is assumed to be rate determining. This leads to a first order back reaction which can be described by :

$$\frac{dc_a}{dt} = -c_a\, A\, \exp\left(\frac{-E_a}{kT}\right) = -c_a\, \gamma D_F\, c_F^{(e)} \tag{2}$$

If the F–centre diffusion coefficient (D$_F$) is $0.01 \exp(-0.8/kT)$ and the mole fraction of F–centres in equilibrium with the colloids ($c_F^{(e)}$) is $2\ 10^{-4} \exp(-0.3/kT)$, an overall activation energy (E$_a$) of 1.5 eV implies that E$_\gamma$ would be 0.4 eV.

In the theoretical models we will assume that the back reaction is first order and that, regarding the discussion above, the probability of the back reaction can be described as $\gamma = 10^{16} \exp(-0.4/kT)$

3.   THE CONVERSION FACTOR BETWEEN DEFECT CONCENTRATIONS AND STORED ENERGY

A problem when comparing the theoretical models with the experimental results is the conversion factor which relates concentrations of defects with stored energy. There is no scientific agreement on the magnitude of this factor. The reported experimental results vary from 4.6 to 12.4 eV per F–H pair corresponding to 75 to 205 J/g per mol% defects. Hughes [1978] gives a theoretical value for this factor of 5.3 eV per F–H pair for free F–centres and 5 eV per F–H pair when the F–centres have agglomerated into colloids. Since there is disagreement among the reported results, we will critically review them and try to understand where the origin of the differences lies. The values given by the various scientists are summarized in Table 1.

Table 1   *Stored energy per F–H pair obtained by various scientists*

Authors	Value (eV/F–H pair)	Experimental techniques	Maximal defect concentration (F–H pairs/cm^3)
Hughes [1978]	5 – 5.3	Theoretical	
Phelps and Pearlstein [1962]	9.2 ± 0.3	L.A., solution calorimetry	7 10^{17}
Bunch and Pearlstein [1969]	12.4 ± 0.3	L.A., D.T.A.	2 10^{18}
Jenks et al. [1975]	4.6	drop calorimetry, H$_2$ and OCl$^-$ measurements	2 10^{20}
Delgado and Alvarez Rivas [1979; 1980]	10	L.A., D.T.A.	4 10^{18}
Groote and Weerkamp [1990]	7.3 ± 0.7	L.A., D.S.C.	10^{20}
Groote and Weerkamp [1990]	9.4	D.S.C. (latent heat – stored energy)	10^{21}
Seinen [1994]	6.2 ± 1	L.A., D.S.C.	10^{20}
Seinen [1994]	5.3 ± 0.5	D.S.C. (latent heat – stored energy)	10^{21}

In his derivation of the theoretical value of the conversion factor Hughes neglected any contribution from the line energy of the dislocation loops. As will be shown below, this approximation is only valid for high damage levels i.e. when the loops are relatively large. The elastic energy of a prismatic dislocation loop (E_l) of radius R can be given by [Hirth and Lothe, 1968]:

$$E_l = \frac{Gb^2R}{2(1-v)} \left[\ln\left(\frac{32R}{b} \right) - 1 \right] \qquad (3)$$
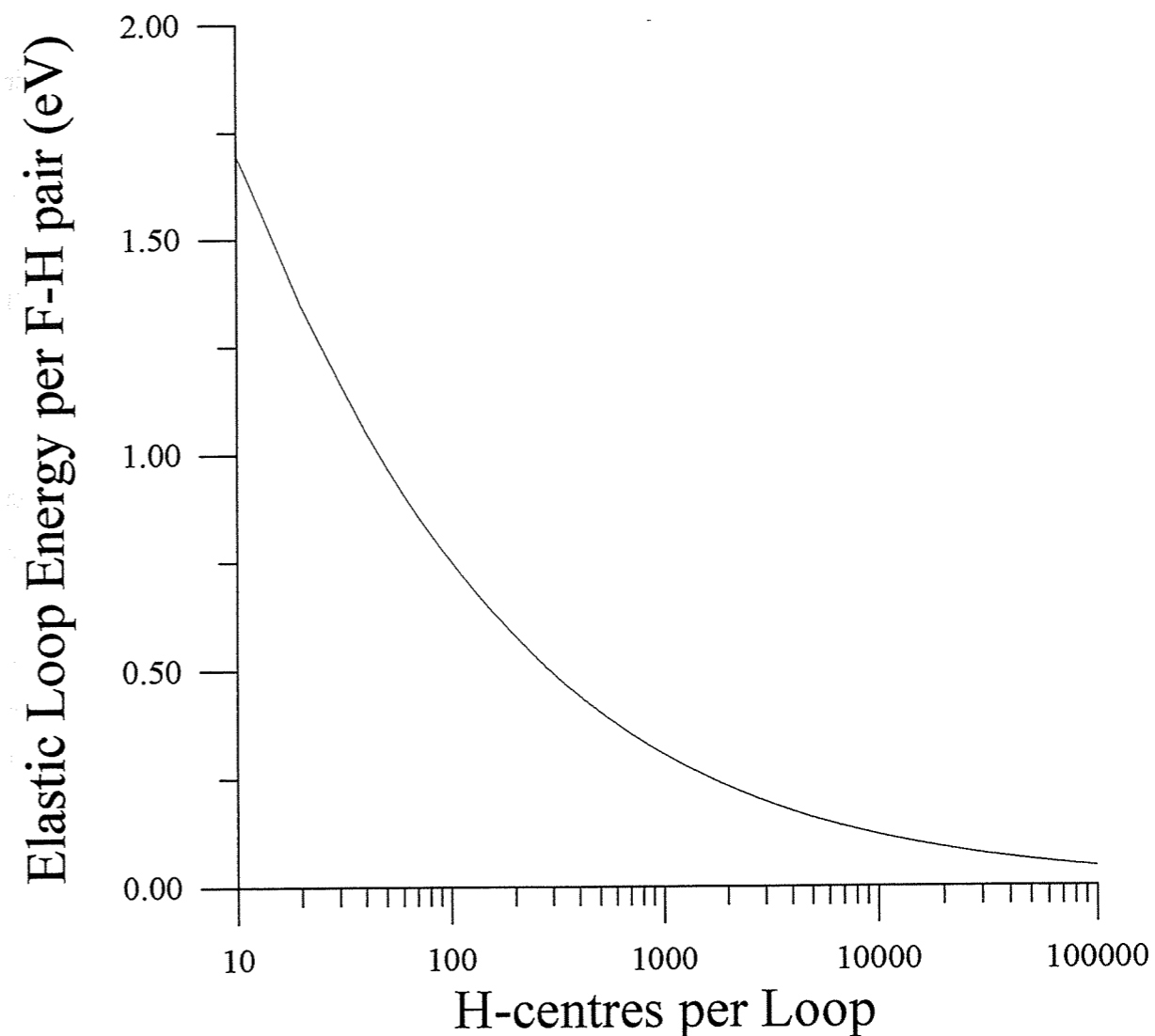
Figure 1:   *Contribution of the elastic loop energy to the stored energy per F–H pair (E_l/N) as a function of the number of H–centres per dislocation loop (N).*

where G is the shear modulus (0.15 Mbar [Simmons and Wang, 1971]), v is Poisson's ratio (0.25 [Simmons and Wang, 1971]) and b the burgers vector of the dislocation (3.98 10^{-8} cm). The radius of the loop will depend on the number of H–centres condensed in the loop (N) and can be approximated by:

$$R = \sqrt{\frac{N}{\sqrt{2}\,\pi}}\, b \qquad (4)$$

This means that the contribution of the elastic loop energy to the stored energy per F–H pair (E_l/N) will depend on the number of H–centres in the loop (N) as:

$$\frac{E_l}{N} = \frac{Gb^3 \sqrt{\dfrac{1}{\sqrt{2}\ \pi}}}{2(1-v)\sqrt{N}} \left[\ln\left(32 \sqrt{\dfrac{N}{\sqrt{2}\ \pi}} \right) - 1 \right]$$

(5)

This dependence is shown in Fig. 1. In this figure it can be seen that the contribution of the elastic energy of the dislocation loops to the stored energy per F–H pair is only negligible when there are more then 1000 H–centres per loop. In the Jain–Lidiard model 10^{15} loops/cm^3 are assumed based on electron microscopy observations of Hobbs. This means that for pure NaCl the contribution of the elastic loop energy is only negligible when the defect concentration is above 10^{18} defects/cm^3. As can be seen from Table 1 this is the case for most of the experiments except those of Phelps and Pearlstein. The experiments of Groote and Weerkamp and Seinen however, have not only been performed on pure but also on doped NaCl samples. According to Hobbs [1973] doping of alkali halides with interstitial trapping impurities leads to an increase in loop density and a decrease of loop size. In the recently published extended versions of the Jain–Lidiard model [Soppe, 1993; Seinen et al., 1992] it is predicted that in doped samples the concentration of dislocation loops can be as high as 10^{17} loops/cm^3. Therefore, it has to be kept in mind that in the derivation of the conversion factor by Groote and Weerkamp and by Seinen from their light absorption measurements a small contribution of dislocation loop elastic energy might have influenced the resulting conversion factor.

The value of 9.2 eV/F–H pair reported by Phelps and Pearlstein contains a correction term of 3.6 eV/F–H pair based on the assumption that on solution of their samples H$_2$ would be produced. De las Cuevas et al. [1992] and Garcia Celma et al. [1993] however, have shown that on solution, of irradiated NaCl containing only F centres and no colloids (as is the case in the experiments of Phelps and Pearlstein), no significant amounts of H$_2$ are produced. The measurements of Phelps and Pearlstein thus lead to a stored energy per defect of 5.6 eV. As stated in the previous paragraph this value also might contain a small contribution from the dislocation loops.

The results obtained by Groote and Weerkamp and those obtained by Seinen are based on the same measurements. The fact that the results of Groote and Weerkamp are higher than those given by Seinen is due to the fact that Groote and Weerkamp made a few errors which have been corrected by Seinen. For instance, a value of 0.0493 eV for the atomic specific heat of melting of sodium was used by Groote and Weerkamp to derive the value of 9.4 eV/F–H pair from their latent heat measurements . The enthalpy of fusion for bulk sodium is 2.598 kJ/mol [Cordfunke and Konings, 1990] leading to a specific atomic heat of 0.027 eV. Using the latter value, Seinen obtained his value of 5.3 eV/F–H pair. On analysing their L.A. measurements Groote and Weerkamp assumed a 50% lorentzian and 50% gaussian line shape for the colloid band. According to Doyle [1958] the colloid band has an approximately lorentzian line shape. Using a lorentzian line shape Seinen obtained a stored energy per F–H pair of 6.2 eV. However, it is unclear in both thesis whether pure or doped samples were used for the L.A. measurements. As stated above if doped samples have been used a small contribution of dislocation loop elastic energy might have influenced the result.

The samples of Phelps and Pearlstein, Bunch and Pearlstein and those of Delgado and Alvarez Rivas were irradiated at room temperature, whereas the samples of the other authors were irradiated at temperatures around 100 °C. In samples irradiated at room temperature only F–centres and no colloids will be present. The difference between the stored energy per F–H pair for free F–centres and F–centres agglomerated into colloids is however, expected to be small (0.3 eV) [Hughes, 1978]

Concluding we can say that all reported values for the conversion factor are approximately equal to the theoretical value of 5 eV/F–H pair except for the values of 12.4 eV/F–H pair reported by Bunch and Pearlstein and 10 eV/F–H pair by Delgado and Alvarez Rivas, which are about twice as large as the other values. Bunch and Pearlstein, however, have measured three stored energy peaks for their irradiated samples. If we only consider the peak at 250 °C, which is ascribed to the anneal of colloids their stored energy per F–H pair amounts to 8.4 eV, which, although still higher, is much closer to the theoretical value of 5 eV/F–H pair. The value reported by Delgado and Alvarez Rivas might be rather inaccurate due to the fact that the F–centre concentration was not determined from the maximum of the F absorption band but calculated from the optical absorption at several wavelengths on the high energy edge of this band. If their reference spectrum contained another absorption at these wavelengths, this would lead to an

overestimation of the result.

The values reported by Bunch and Pearlstein and Delgado and Alvarez Rivas are larger than the energy of lowest exciton state 7.9 eV (and even larger than the bandgap) of NaCl and are therefore inconsistent with the now generally accepted excitonic formation mechanism of the F and H centres [Itoh, 1982]. The high values reported by Bunch and Pearlstein and Delgado and Alvarez Rivas can only be explained by the presence of some other kind of defects than those mentioned in the introduction of this paper. We have not found convincing experimental evidence for the existence of other defects than F and H centres and their related agglomerates. Therefore, it is not clear why Bunch and Pearlstein and Delgado and Alvarez Rivas found such high values for the conversion factor. We, however, conclude that for the conversion of concentration of defects into stored energy a value of about 5 eV/F–H pair should be used.
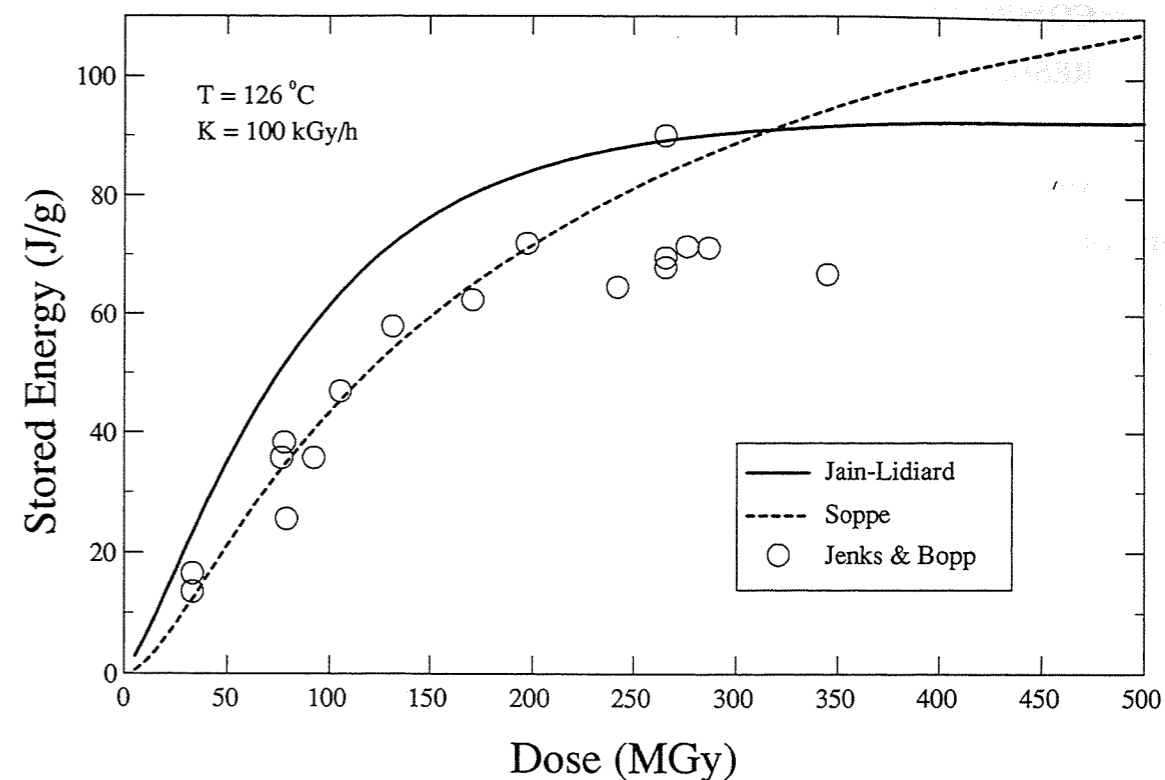

Figure 3: *Comparison of predicted stored energy values according to the Jain–Lidiard model and according to Soppe's model with experimental results obtained by Jenks and Bopp at 126 °C. Dose rate 100 kGy/h.*
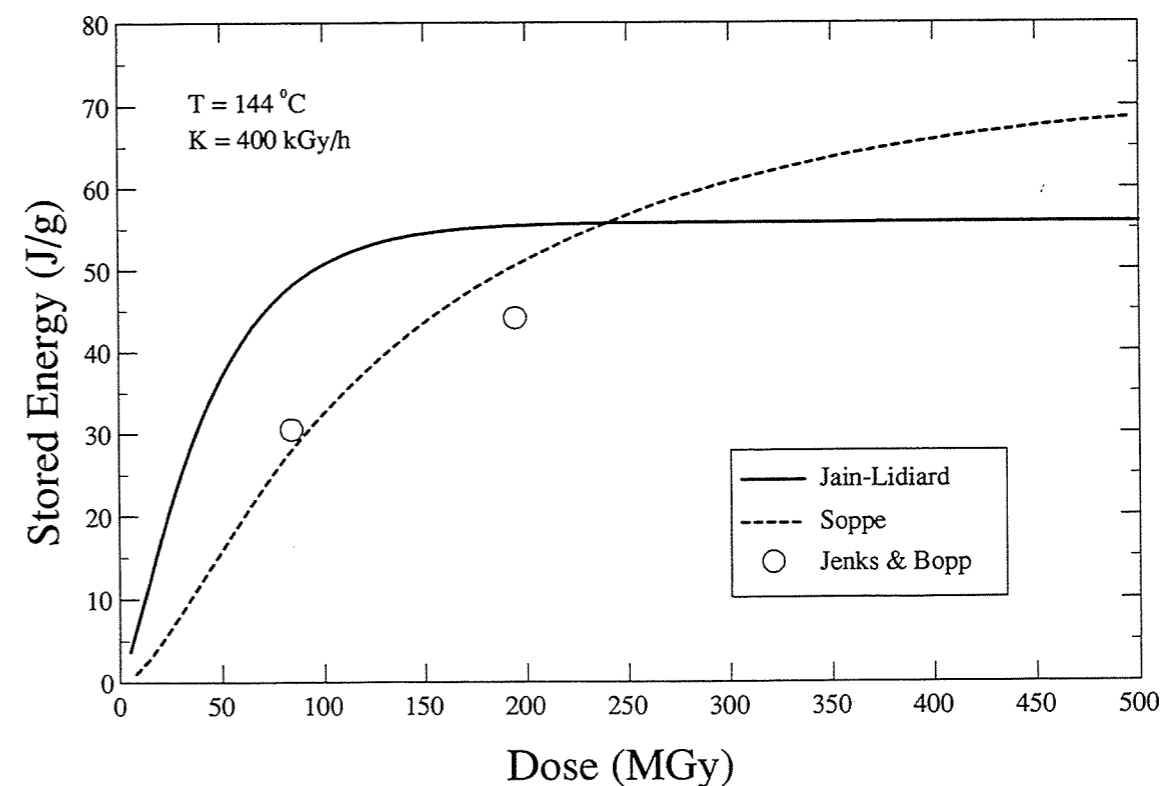

Figure 2: *Comparison of predicted stored energy values according to the Jain–Lidiard model and according to Soppe's model with experimental results obtained by Jenks and Bopp at 95 °C. Dose rate 100 kGy/h.*

Figure 4: *Comparison of predicted stored energy values according to the Jain–Lidiard model and according to Soppe's model with experimental results obtained by Jenks and Bopp at 144 °C. Dose rate 100 kGy/h.*

4. COMPARISON OF THE MODIFIED MODELS WITH THE EXPERIMENTAL RESULTS OF JENKS AND BOPP

With the modifications discussed in the previous chapters both models were compared with the experimental results obtained by Jenks and Bopp [1974; 1977]. For the Jain–Lidiard model a satisfactory agreement between model calculations and these experiments was obtained as can be seen in Fig. 2 to 4. For the model of Soppe a satisfactory agreement between calculations and experiment could only be obtained if the maximum dislocation density was increased by a factor two i.e. $\rho_m = 2\, C_I^{2/3}$ which is in between the value suggested by Lidiard [1979] $\rho_m = C_I^{2/3}$ and the value used by Seinen et al. [1992; 1994] $\rho_m = (6\pi^2\, C_I^2)^{1/3}$. With this increased value for ρ_m there is a reasonable agreement between the model calculations and the experiments as can also be seen in Fig. 2 to 4.
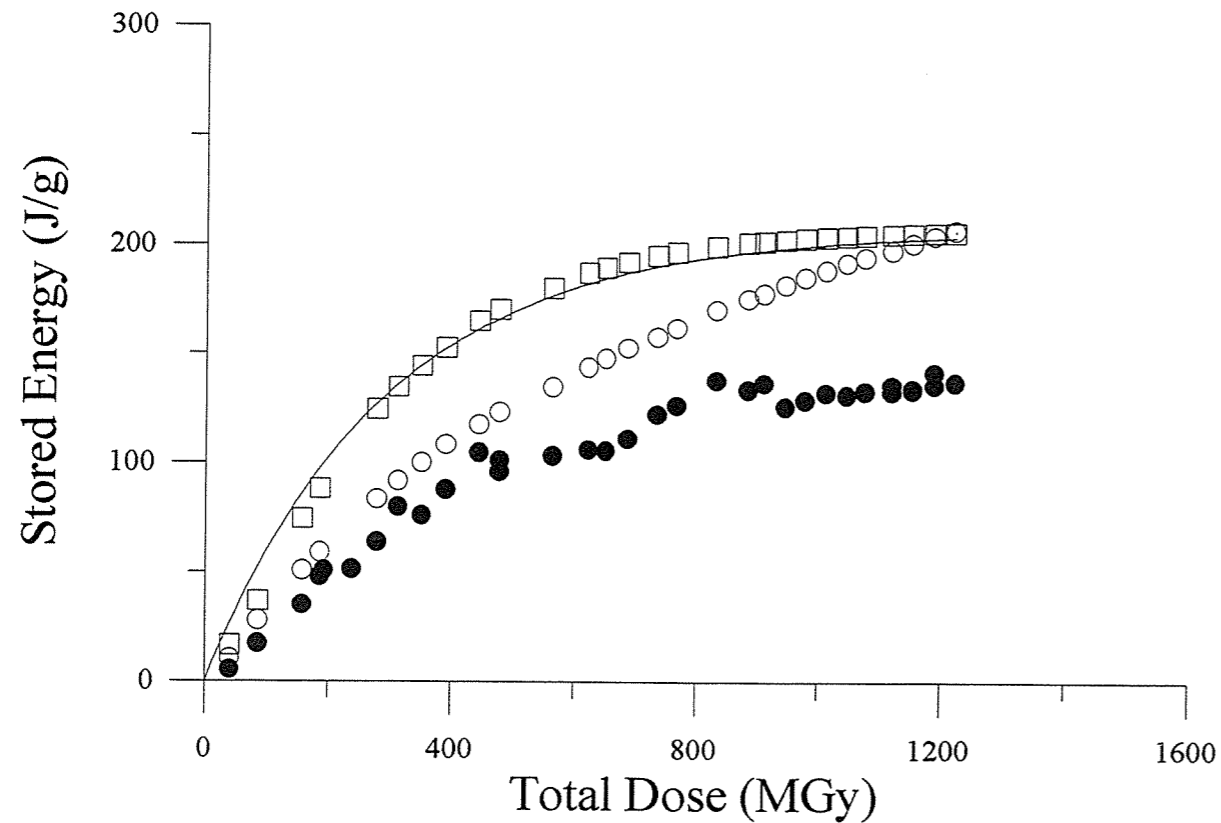

Figure 5: *Comparison of measured stored energy values on irradiated Sp–800 samples (full circles) with model calculations using the modified Jain–Lidiard model (open squares) and with model calculations using the extended Jain–Lidiard model by Soppe (open circles). The drawn line is a prediction of the damage according to Eq. (6) (see text)*

5. COMPARISON OF THE MODIFIED MODELS WITH SP–800 SAMPLES IRRADIATED IN GIF A

In Fig. 5 the stored energy data obtained for the Sp–800 samples irradiated in GIF A [Donker and Garcia Celma, 1995] are compared with predictions obtained from simulating our experiments with the models as mentioned and modified in the previous chapters. Since we do not know the impurity content of our samples we have used the model of Soppe for pure salt. In Fig. 5 it can be observed that the values predicted by the model are higher than those experimentally observed. At low total doses the predictions obtained from the model of Soppe are closer to the experimental data then the Jain–Lidiard model. The Jain–Lidiard model, however, qualitatively agrees with the experiment in respect to the occurrence of a saturation level for the stored energy at high doses. The model of Soppe does not predict a saturation level at the studied total doses.

In Fig. 2 to 4 it can be observed that at least the Jain–Lidiard model and to a less extent also the model of Soppe slightly overestimate the experimental results of Jenks and Bopp at high doses. According to the Jain–Lidiard model the colloid fraction for large irradiation times can be approximated by [Soppe et al., 1994]:

$$c_A(t) = c_A^{(sat)}\, (1 - \exp(-\alpha\, t)) \qquad (6)$$

where

$$c_A^{(sat)} = \frac{\rho_d^{(max)}}{\gamma}\left[(z_H - z_F) - z_H\frac{c_F^{(e)}}{c_F^{(sat)}}\right] \qquad (7)$$

and

$$\alpha = \frac{4\pi r_c C_c D_F}{4\pi r_c C_c + z_H \rho_d}\gamma\, c_F^{(sat)} \qquad (8)$$

For large irradiation times $z_H\rho_d \ll 4\pi r_c C_c$ and α can be approximated by:

$$\alpha = D_F \gamma c_F^{(sat)} \tag{9}$$

The solid line in Fig. 5 is a prediction of the stored energy in our Sp–800 samples using Eq. 6 and the average dose rate in our experiments, i.e. 44 kGy/h and all the other parameters the same as in the Jain–Lidiard model. As can be seen this prediction practically coincides with the predictions obtained from simulating the experiments with the full Jain–Lidiard model (squares in Fig. 5).It can be shown that a similar coincidence occurs when simulating the experiments of Jenks and Bopp.

According to Eq. 7 the saturation value for the colloid fraction is mainly determined by $\rho_d^{(max)}$, γ and $(z_H - z_F)$. This will also hold for the full models. All three terms are not known very accurately. It is therefore surprising that the agreement between the models and the experiments is that good. It is however possible that with another choice of parameters, within their physically known accuracy, an equally good or even better correspondence can be obtained. If for instance the activation energy for the back reaction E_γ is decreased from 0.4 to 0.39 eV, $c_A^{(sat)}$ in Eq. 7 for our experiment decreases from 200 to 150 J/g yielding a much better correspondence with our experimental result. We, however, refrain from making this parameter change in the models for several reasons. Firstly, on doing so we would suggest an accuracy that is not real. The experiments of Seinen and our DTA scans show that the back reaction depends heavily on sample composition. At this moment it cannot even be excluded that the mechanism or rate determining step of the back reaction is different for different sample compositions. Secondly, an equally good correspondence between model and experiment could be obtained from modifying $\rho_d^{(max)}$ and/or $(z_H - z_F)$.Thirdly, the differences between model predictions and experiments might very well not be due to the parameterisation of the models but due to the fact that in the samples certain processes occur that are not yet included in the models. Our conclusion about the accuracy and reliability of the models can therefore not go further than that the model predictions are of the same order of magnitude as the experimental results and that they at least do not give an underestimation of the experimental results.

6. CONCLUSIONS

The discussions above shows that not to much can be said about the reliability of the model predictions under repository conditions. At this moment regarding the present results, our feeling is that it is very unlikely that the model predictions for a repository will give an underestimation of the damage. Also because some anneal mechanisms which we have observed in our experiments and of which we expect that they will increase in importance when the dose rate decreases have not yet been included in the theoretical models. To certify our statement however, more or more accurate information about certain parameters in the models and a theoretical inclusion of the mentioned anneal mechanisms is necessary. Also a sensitivity analysis to determine which model parameters are essential for the predictions for a repository is called for. On the experimental side we can say that at least more research into the nature of the back reaction and a determination of the maximum dislocation density is necessary.

REFERENCES

J.M. BUNCH and E. PEARLSTEIN, 1969: "*Stored Energy in Irradiated Sodium Chloride*", Phys. Rev. **181**, 1290–1297.

E.H.P. CORDFUNKE and R.J.M. KONINGS, 1990: in "Thermochemical Data for Reactor Materials and Fission Products", Elsevier, Amsterdam, p. 326

C. DE LAS CUEVAS and P. TEIXIDOR, 1992: "*Colloidal Sodium Determinations, Work Performed by ENRESA*" in "The HAW–project: Test Disposal of Highly Radioactive Radiation Sources in the Asse Salt Mine, Summary Report May 1990 – December 1991", GSF Bericht – 8/92, GSF – Forschungszentrum für Umwelt und Gesundheit, GmbH, Neuherberg, p. 173 – 203.

L. DELGADO and J.L. ALVAREZ RIVAS, 1979: "*Stored Energy and Thermoluminescence in NaCl Irradiated at Room Temperature*", J. Phys. C: Solid State Phys. **12**, 3159–3167.

L. DELGADO and J.L. ALVAREZ RIVAS, 1980: "*Stored Energy in Alkali Halides Irradiated at Room Temperature*", J. Phys. C: Solid State Phys. **13**, 1185–1196.

H. DONKER and A. GARCIA CELMA, 1995: "*On the Saturation of Radiation Damage in Irradiated Natural Rock Salt*", article 18 in this volume.

W.T. DOYLE, 1958: "*Absorption of Light by Colloids in Alkali Halide Crystals*", Phys. Rev. **111**, 1067–1072.

A. GARCIA CELMA, C. DE LAS CUEVAS, P. TEIXIDOR, L. MIRALLES and H. DONKER, 1993: *"On the Possible Continuous Operation of an Intergranular Process of Radiation Damage Anneal in Rock Salt Repositories"* in "Geological Disposal of Spent Fuel and High Level and Alpha–Bearing Wastes, Proceedings of a Symposium, Antwerp, 19–23 October 1992", International Atomic Energy Agency, Vienna, p. 133–144.

J.C. GROOTE and J.R.W. WEERKAMP, 1990: *"Radiation Damage in NaCl; Small Particles"*, Thesis, Groningen University, 270 p.

J. P. HIRTH and J. LOTHE, 1968: *"Theory of Dislocations"*, (McGraw–Hill, New York) p. 145.

L.W. HOBBS, 1973: *"Transmission Electron Microscopy of Defects in Alkali Halides"*, J. Physique **34** C9, 227–241.

A.E. HUGHES, 1978: *"Annealing of Irradiated Alkali Halides"*, Comments Solid State Phys. **8**, 83–92.

N. ITOH, 1982: *"Creation of Lattice Defects by Electronic Excitation in Alkali Halides"*, Adv. Phys. **31**, 491–551.

U. JAIN and A.B. LIDIARD, 1977: *"The Growth of Colloidal Centres in Irradiated Alkali Halides"*, Phil. Mag. **35**, 245–259.

G.H. JENKS and C.D. BOPP, 1974: *"Storage and Release of Radiation Energy in Salt in Radioactive–Waste Repositories"*, Oak Ridge Natn. Lab. Rep., ORNL–TM–4449, 77 p.

G.H. JENKS and C.D. BOPP, 1977: *"Storage and Release of Radiation Energy in Salt in Radioactive–Waste Repositories"*, Oak Ridge Natn. Lab. Rep., ORNL–5058, 97 p.

G.H. JENKS, E. SONDER, C.D. BOPP, J.R. WALTON and S. LINDENBAUM, 1975: *"Reaction Products and Stored Energy Released from Irradiated Sodium Chloride by Dissolution and by Heating"*, J. Phys. Chem. **79**, 871–875.

A.B. LIDIARD, 1979: *"Energy Stored in Irradiated NaCl"*, Phil. Mag. **A39**, 647–659

G. VAN OPBROEK and H.W. DEN HARTOG, 1985: *"Radiation Damage of NaCl: Dose Rate Effects"*, J. Phys. C: Solid State Phys. **18**, 257–268

F.T. PHELPS and E. PEARLSTEIN, 1962: *"Measurement of the Stored Energy in X–Rayed Sodium Chloride"*, Phys. Rev. **128**, 1575–1585.

J. SEINEN, 1994: *"Radiation Damage in NaCl: the process of colloid formation"*, Thesis, Groningen University, 142 p.

J. SEINEN, J.C. GROOTE, J.R.W. WEERKAMP and H.W. DEN HARTOG, 1992: *"Radiation Damage in NaCl: General Model of Nucleation and Aggregation Processes in Doped NaCl"*, Rad. Eff. Def. Solids **124**, 325–339.

G. SIMMONS and H. WANG, 1971: *"Single Crystal Elastic Constants and Calculated Aggregate Properties: A Handbook"*, (M.I.T. Press, Cambridge, Massachusetts) p. 271.

W.J. SOPPE, 1993: *"Computer Simulation of Radiation Damage in NaCl by using a Kinetic Rate Reaction Model"*, J. Phys.: Condensed Matter **5**, 3519–3540.

W.J. SOPPE, H. DONKER, A. GARCIA CELMA and J. PRIJ, 1994: *"Radiation Induced Stored Energy in Rock Salt"*, J. Nuc. Mat. **217**, 1–31.

THE EFFECT OF CRYSTAL DEFECT DENSITY GRADIENTS ON RADIATION DAMAGE DEVELOPMENT AND ANNEAL.

A. García Celma , W. Soppe and H. Donker

ABSTRACT

Some modifications on the classical radiation damage simulation model developed by Jain and Lidiard are here presented. They simulate the effect on radiation damage of gradients of dislocation concentration, impurity concentrations, and radiation dose rate. With these modifications the heterogeneous colour distribution due to incipient colloid development observed in the microstructures of irradiated salt samples can be explained

1. INTRODUCTION

The primary defects formed during irradiation of NaCl are F- and H-centres. These complementary defect centres can, however, easily recombine, restoring the NaCl lattice. To produce permanent radiation damage these primary point defects have to be kept from recombining. In a perfect lattice, however, stabilizing point defects would be very difficult. Following Hobbs [1972], if dislocations are present, H-centres can be stabilized via a mechanism in which two H-centres "dig out" a NaCl ion pair from its regular position and form a Cl_2 molecule. The NaCl ion pair moves to the extra plain of the dislocation. Hobbs et al. [1973] also observed that during irradiation perfect edge dislocation loops in the [011] planes are formed. According to the mechanism described above, H-centres can be stabilized in places above and below (nearby and within the projection of) these dislocation loops. How the nucleation of these dislocation loops proceeds has however not been clarified. To circumvent this problem, in the theoretical models describing the radiation damage formation, it was either assumed that the dislocation loops already existed [Jain and Lidiard, 1977] or that other H-centre trapping

distortions (together with the H–centres) collapsed into dislocation loop structures [Seinen et al., 1992; Soppe, 1993]. Hobbs [1976] considered the distortion field around Na^+ lattice positions substitutionally occupied by divalent cation impurities as the most likely places for the nucleation of dislocation loops.

All models and theories assume the crystals to be homogenous entities since they disregard spatial distributions and perform calculations using only time–dependant concentration values. The general form of the mass balance of a given defect X, however, is:

$$\frac{\partial c_X}{\partial t} = Q_X^{source} - Q_X^{sink} + D_X \nabla^2 C_X \qquad (1)$$

In the theoretical models developed so far it is assumed that the salt is homogeneous and that there are no gradients in the concentrations of the various defects; i.e. the last term of (1) is zero. In the Jain–Lidiard model thus :

$$Q_F^{source} = K + 4\pi r_C C_C D_F c_F^{(e)} \qquad (2)$$

i.e. the production rate of F–centres (Q_F^{source}) is equal to their direct production rate (K) plus that of their evaporation from colloids ($4\pi r_c C_c D_F c_F^{(e)}$). On the other side, the F–centres concentration in solution diminishes (by an amount Q_F^{sink}) through recombination with H–centres, trapping at dislocation lines, recombination with Cl_2 molecules, and precipitation in the form of colloids. This is respectively represented by each term in (3)

$$Q_F^{sink} = K_2 c_F c_H + z_F \rho_d D_F c_F + \gamma D_F c_F c_A + 4\pi r_C C_C D_F c_F \qquad (3)$$

Similar expressions can be written for the H–centres, except that, for these centres, it is assumed that their precipitates in the form of Cl_2 are stable and therefore no H–centra evaporate from them. Taking into account this assumption the production rate of H centres is:

$$Q_H^{source} = K \qquad (4)$$

And the rate at which H–centres are taken out from the solution, which depends on similar processes as that of the F centres, is expressed as in (5)

$$Q_H^{sink} = K_2 c_F c_H + z_H \rho_d D_H c_H + 4\pi r_C C_C D_H c_H \qquad (5)$$

Then Jain and Lidiard define the rate of colloid production as the rate of sinking in of F centres :

$$Q_A^{source} = 4\pi r_C C_C D_F c_F \qquad (6)$$

And the rate of colloid annihilation as the evaporation rate of F centres from colloids plus the rate of H–centre recombination with colloids:

$$Q_A^{sink} = 4\pi r_C C_C D_F (c_F^{(e)} + c_H) \qquad (7)$$

As stated above, in the equations written by Jain and Lidiard it is assumed that the salt is homogeneous and that there is no variation in concentration of defects, nor gradients driving diffusion. However, something else than just random diffusion and random fixation of H–centres near randomly distributed impurities has to be envisaged if radiation damage has to be explained. Moreover randomness can never explain the heterogeneous colour distribution observed in irradiated samples.

In natural rock salts, intra en intercrystalline heterogeneities, all with extensions larger than some crystal lattice cells are always present and can be assumed to create gradients in defect concentrations which would drive diffusion in a preferent direction. Reinforcement of the concentration of a given colour centre (H– or F–centre) could then take place, but, since both (complementary) defects could be driven to diffuse in the same direction, annihilation could as
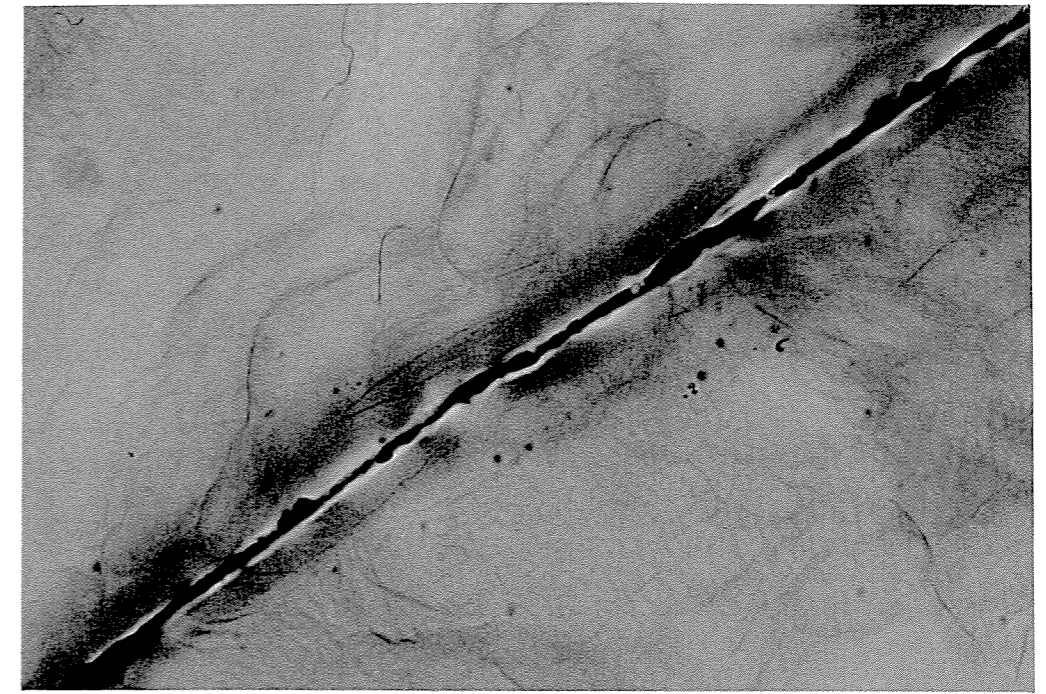
Figure 1   *Micrograph of a natural rock salt sample irradiated up to 2.6 MGy at 15 kGy/h and 100 °C. The black structure crossing the micrograph from top−right to bottom−left is a grain boundary void. Observe the colourless rim limited by the intense blue rim. The other colloid decorated structures are cellular patterns and incipient subgrain boundaries. Magnification 338 X.*
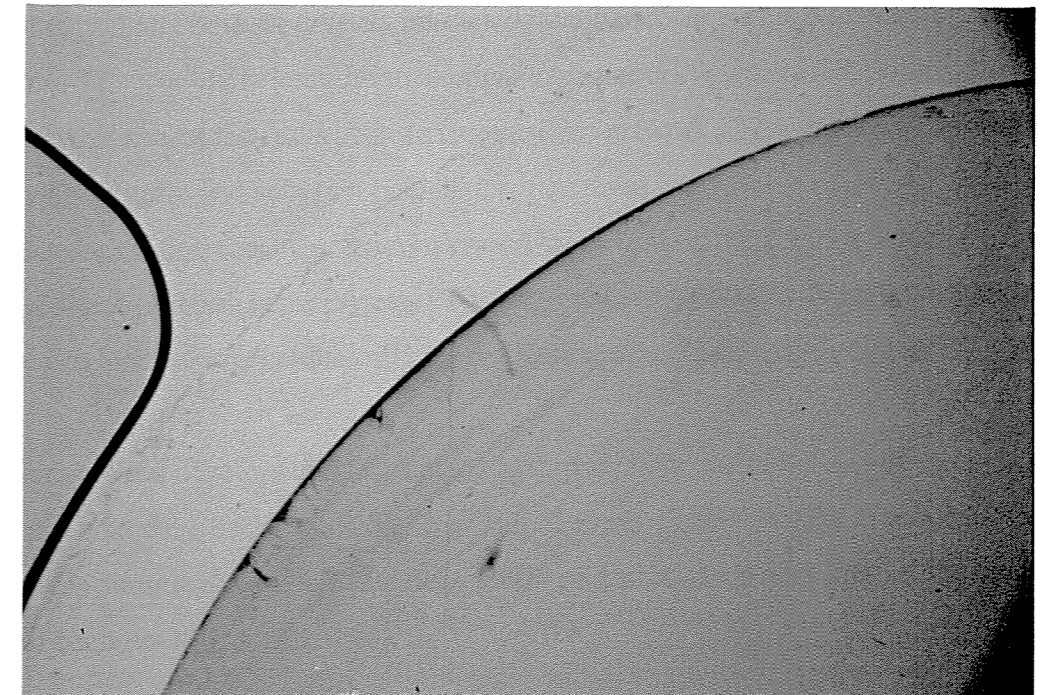

Figure 2   *Micrograph of a pure undeformed single crystal of NaCl irradiated up to 4 MGy at 15 kGy/h and 100 °C. Observe the dark colloid decorated, circular crystal outer surface. The outermost surface is too thin to be observed in this photograph but can be observed in Fig. 3. Magnification 34 X.*

well be the result. Both constructive and destructive results have been observed in the colour distribution. We try to obtain the "calculated" equivalents of the damage heterogeneity observed in the experiments through modelling the heterogeneities previous to the irradiation and the effect we believe they have on point defect dynamics. If the models reproduce the "heterogeneities" they would constitute a good test on our radiation damage development understanding.

As a basis we will use expression (1) for the mass balance of a defect X. Notice that in (1) a variation on the defect gradient ($D_x\nabla^2C_x$) is introduced which is never taken into account in the Jain–Lidiard model.

2. EXPERIMENTAL OBSERVATIONS

Intracrystalline distribution of damage is not homogeneous, but controlled by dislocation substructures. This is observed both on natural samples and on pure undeformed single crystals (Harshaw). It has been observed [Donker and García Celma, 1995] that rock salts do not contain more stored energy than Harshaw crystals irradiated simultaneously with them and under the same conditions. This contradiction with theoretical expectations is attributed, amongst other causes, to the fact that natural rock salts posses a more extense network of exterior crystal surfaces (sample boundaries, grain and subgrain boundaries, fractures) per volume of sample than the Harshaw crystals do, a higher density of exterior crystal surfaces would enhance creep due to the development of defect gradients in the crystals. The creep will take place associated with anneal even when the original heterogeneities will ease nucleation of radiation damage defects.

Incipient colloid development takes place near grain boundaries but at a distance from them. The grain boundary itself is colloid–free and at some distance to the exterior surface colloids appear constituting a dark blue line from which on and towards the centre of the crystal the blue colour becomes lighter (Fig. 1–3).

At a lower scale, the blue colour produced by the colloids is observed to display patterns which can be recognized as dislocation substructures. Most of these substructures were not present before irradiation and therefore are produced by the irradiation itself. The substructures grade from incipient slip bands (Fig. 3) , to well developed cross slip structures, subgrain
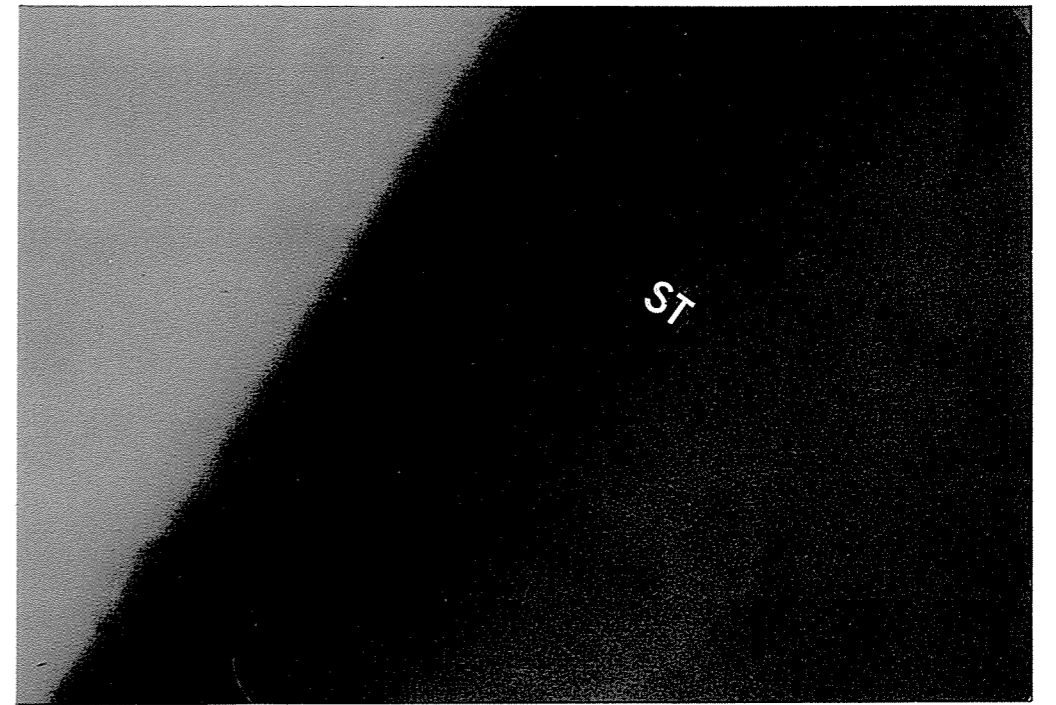
Figure 3   *Blow up of the dark rim of Fig.2. There is a colourless outer rim of the crystal which is seen as a less blue blurred rim at this magnification. The direction of incipient slip traces (ST) is indicated. The blue rim is made up of these incipient slip traces. Magnification 1343 X.*
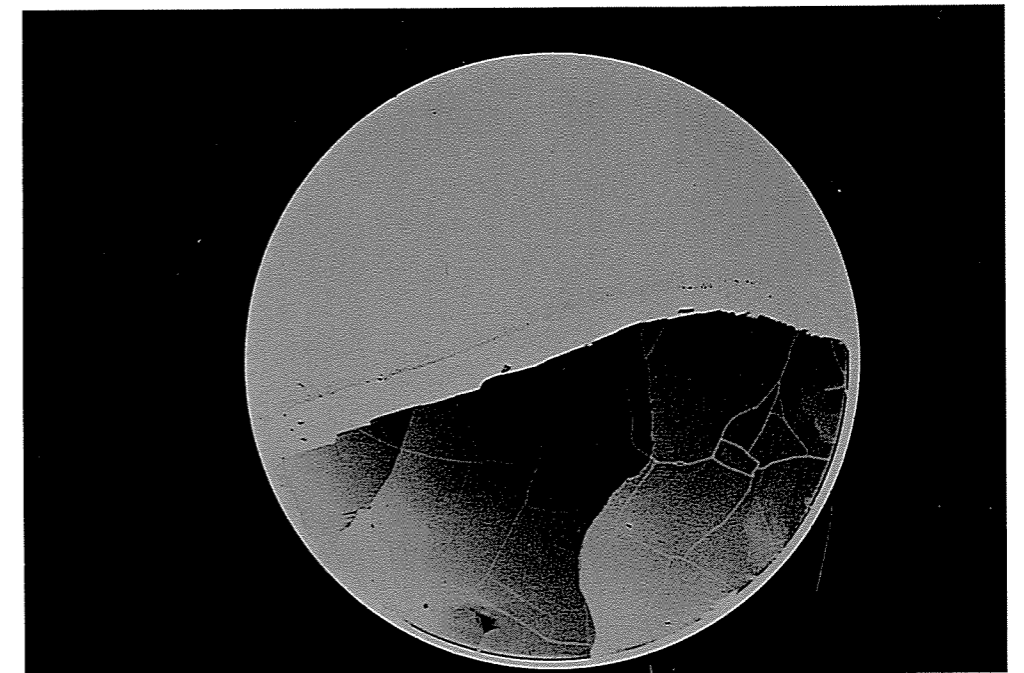

Figure 4   *Micrograph of a pure undeformed NaCl crystal irradiated up to 24 MGy at 15 kGy/h and 100 °C. The different darkness of parts of the crystal are a thin section preparation artifact. The colourless (white) lines network is a subgrain boundary network developed during irradiation. Magnification 4 X.*

Figure 5   *Micrograph of a natural rock salt sample irradiated up to 2.6 MGy at 15 kGy/h and 100 °C. Subgrain boundaries developing by climb of colloid decorated cross slip structures (cellular patterns), while near the polyhalite (P) boundary with the halite som of the subgrain boundaries already constitute a preferred diffusion path (incipient discolouration can be observed). Magnification 338 X.*

boundaries produced by dislocation climb processes (Fig. 4) and new grain boundaries of high surface equilibrium produced by polygonization due to further progression of this creep [García Celma and Donker, 1994]. Notice that since we observe them because they are blue, this means that when the dislocation migrate to constitute the various different arrangements the colloids are either destroyed and re-nucleated or migrate together with the creep structures.

Those substructures which are material discontinuities are observed as a white rim limited by a blue rim with the same structure as observed for incipient colloid development (see Fig. 5,6). If the material discontinueties were already present in the sample at the beginning of the irradiation it can be assumed that colloids did not develop at the exterior surface as is the case with Harshaw single crystals. However, if they are produced by creep during irradiation by dislocation wall development (e.g. subgrain boundaries) (Fig. 4) it has to be assumed that bleaching took place since dislocation lines are first blue. An extreme example of this colloid distribution was obtained in the Brine Migration Test [Gies et al.,1994] (see Fig. 7).

3. HETEROGENEOUS DISLOCATION DISTRIBUTION

Natural rocks compact by adaption to the strain (deformation) produced by the overlying pack of rocks. When stress results in plastic deformation, dislocations and their arrangements are the lattice expression of the strain undergone by the rock. Dislocations in deformed materials mostly display a core-mantle distribution. This means that the mantles of the crystals protect their inner parts (the cores) from the action of externally applied deformation through plastically adapting themselves to the deformation, and thus accumulate dislocations.

Therefore, the dislocation density at the mantle is many times bigger than at the core of any crystal. Lets thus assume a spherical grain with radius R where the distribution of the dislocations is described by:

$$\rho_d(r,t) = \rho_d e^{-\kappa(R-r)} \tag{8}$$

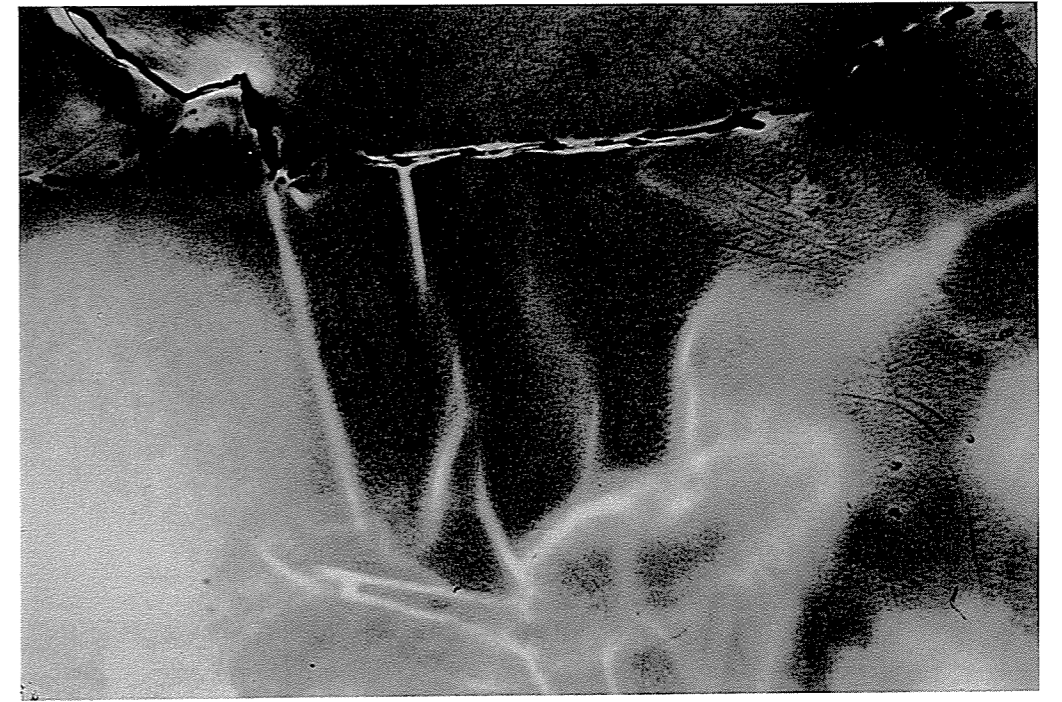Since we may assume that the concentration of the H centres is steady ($\delta c_H/\delta t = 0$), the

Figure 6   *Micrograph of a natural rock salt sample irradiated up to 4 MGy at 15 kGy/h and 100 °C. Well developed subgrain boundaries ending at a grain boundary, all bleached by preferred diffusion of radiation damage defects towards the grain boundary void. Magnification 338 X.*
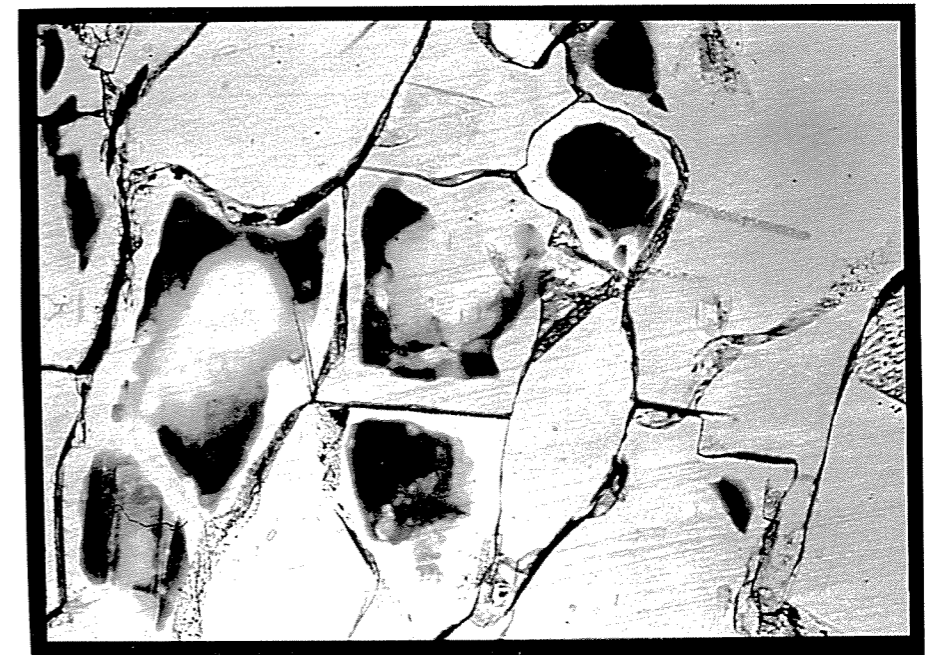

Figure 7   *Micrograph of a natural rock salt sample from the Brine Migration Test (in situ irradiation experiment at the Asse Mine). Observe the very exaggerated white (colourless) rims near the grain boundaries and the blue rims fading towards the grain cores. Magnification 7 X.*

contribution of the diffusion of H centres is easy to determine if we also assume that it is a second order effect. We can then write:

$$\nabla^2 c_H = \nabla^2 \left(\frac{K}{K_2 c_F + z_H \rho_D D_H + D_H 4\pi r_C C_C} \right)$$

$$= \frac{1}{r^2} \frac{\partial}{\partial r} (r^2 \frac{\partial}{\partial r}) \frac{K}{A + B\rho_d(r,t)} \qquad (9)$$

where $A = K_2 c_F + 4\pi r_c C_c D_H$, and $B = z_H D_H$, equation (9) then gives:

$$\nabla^2 c_H = -\frac{\kappa K B \rho_d(r,t)}{(A + B\rho_d(r,t))^2} \left[\frac{2}{r} + \kappa - \frac{2\kappa B \rho_d(r,t)}{A + B\rho_d(r,t)} \right] \qquad (10)$$
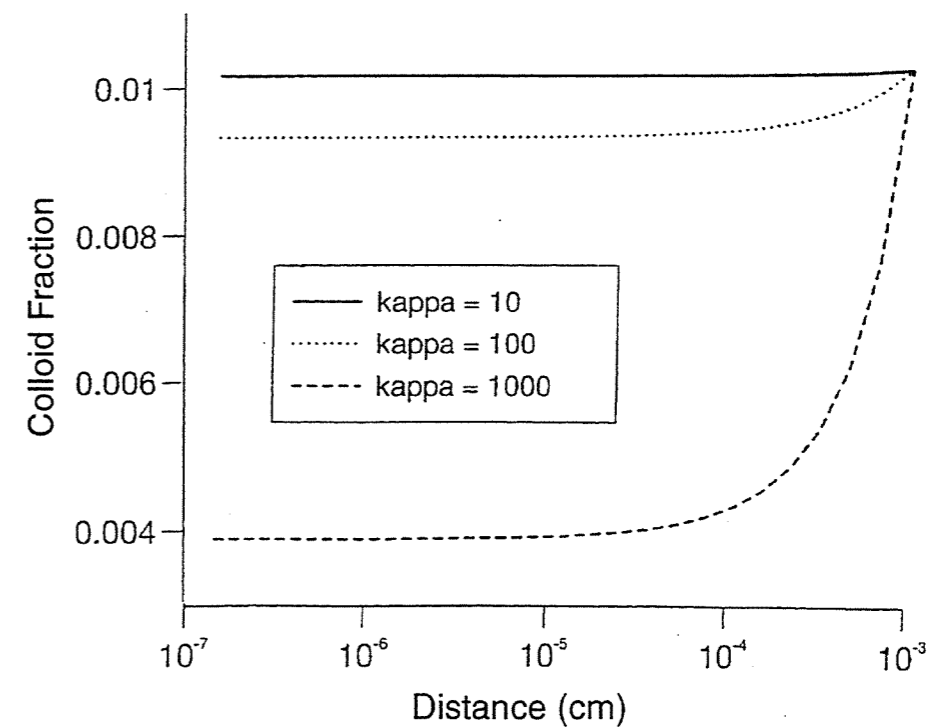
Figure 8   Calculated colloid fraction as a function of distance from the grain core for a spherical grain of radius 10^{-3} cm, assuming a heterogeneous dislocation distribution (see text). Dose rate 100 kGy/h, total dose 833 MGy

374

The diffusion term for the F–centres is more difficult to consider because we do not have any analytical expression for their concentration as a function of crystal radius and time. We have tried some approximations but they all lead to difficulties in integrating $\partial c_F / \partial t$. If the diffusion term for the F–centres is not considered and the heterogeneities are only expressed using (8), the differential equations for c_F and c_H could be integrated. The results of the model for three different values of κ are represented in Fig. 8. The value assumed for the dose rate K was 100 kGy/h, and the total dose 833 MGy. It can be seen that in these simulations the colloid fraction follows more or less the behaviour of the dislocation line density: a maximum concentration at the grain boundary and an exponential decrease in the direction of the grain core.

4.   THE EFFECT OF THE GRAIN BOUNDARY

In the previous chapter we have shown that we can explain that regions of the crystals where many dislocations are present develop more radiation damage than regions with lower dislocation densities. In natural rock salts the highest dislocation densities are expected at the grain boundaries. However, the first place where colloids develop in natural samples is not at but near the grain boundaries and in Harshaw crystals near the crystal boundary. The crystal/grain boundaries themselves tend to be devoid of colloids while the colloids are observed in the optical microscope as accumulating at a given distance between 2 and 7 microns of the free surface of the crystal/grain. Towards the crystal/grain interior the colloid concentration gradually diminishes. See the micrographs in Fig. 1–3.

One of the most important differences with a perfect crystal (as assumed in the models) displayed by the crystals used in our experiments is that the real crystals are finite and that they have exterior surfaces. The exterior surfaces can be described as an accumulation of dislocations. To simulate the grain boundary we considered that there are three dislocation lines per unit cell at the exterior surface of the grain, and that the dislocation density is many times bigger at the mantle than at the core of an halite crystal. We have approximated this by the following expression:

$$\rho = \rho_1 \, e^{-\kappa(R-r)} + \rho_d \qquad (11)$$

in which r is the distance from the grain boundary, ρ_1 is the dislocation density at the surface and ρ_d is the dislocation density in the bulk of the crystal. Notice that this expression is very similar to Eq. (8). The main difference, however is that the dislocation density at the surface is now many orders of magnitude higher than in (8)

Using Eq. (11) the Jain–Lidiard model gives the colloidal distribution displayed in Fig. 9. In Fig. 9 the dose rate K= 100 kGy/h ; total dose simulated was 833 MGy, $\kappa = 10^4$ cm^{-1}, and $\rho_1 = 10^{12}$ cm^{-2}. From Fig. 9 it can be observed that the colloid distribution predicted by the model agrees with the experimental observations, i.e. the model predicts that a maximum colloid concentration will occur at a few microns from the surface of the crystal/grain and that the surface itself will be devoid of colloids.
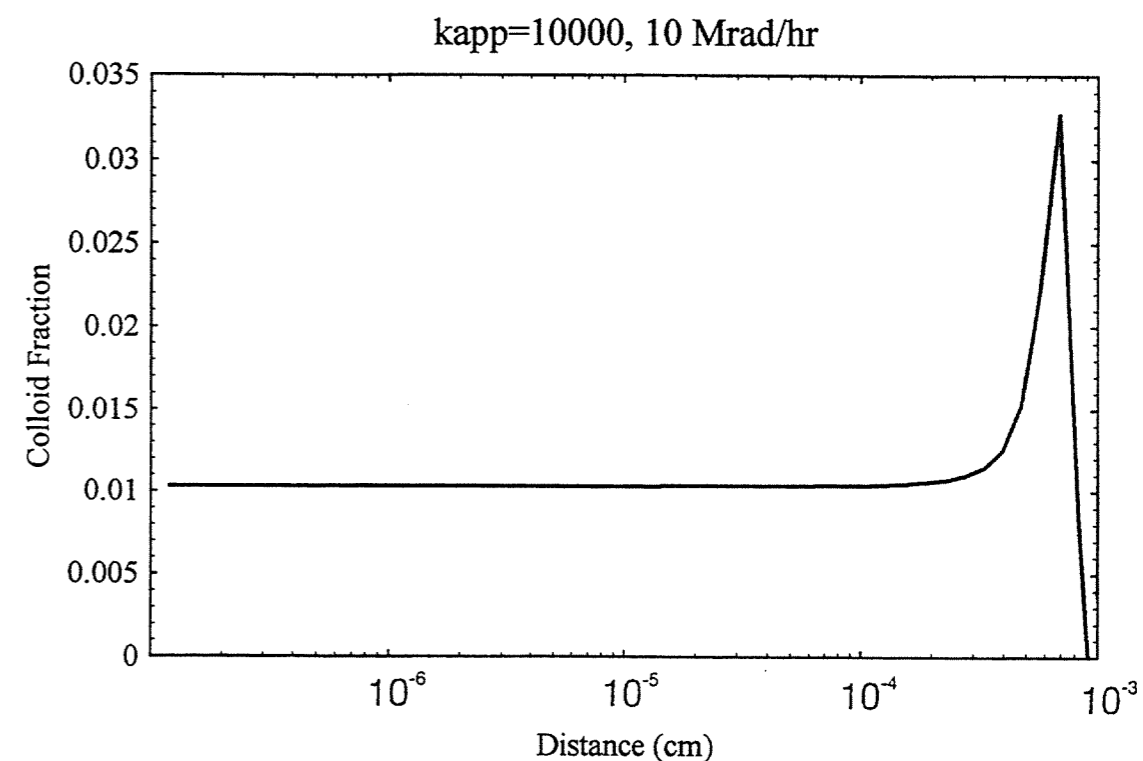
Figure 9   *Calculated colloid fraction as a function of distance from the grain core for a spherical grain of radius 10^{-3} cm, assuming a dislocation distribution according to Eq. 11 (see text). Dose rate 100 kGy/h, total dose 833 MGy, $\rho_1 = 10^{12}$ cm^{-2} and $\kappa = 10^4$ cm^{-1}.*
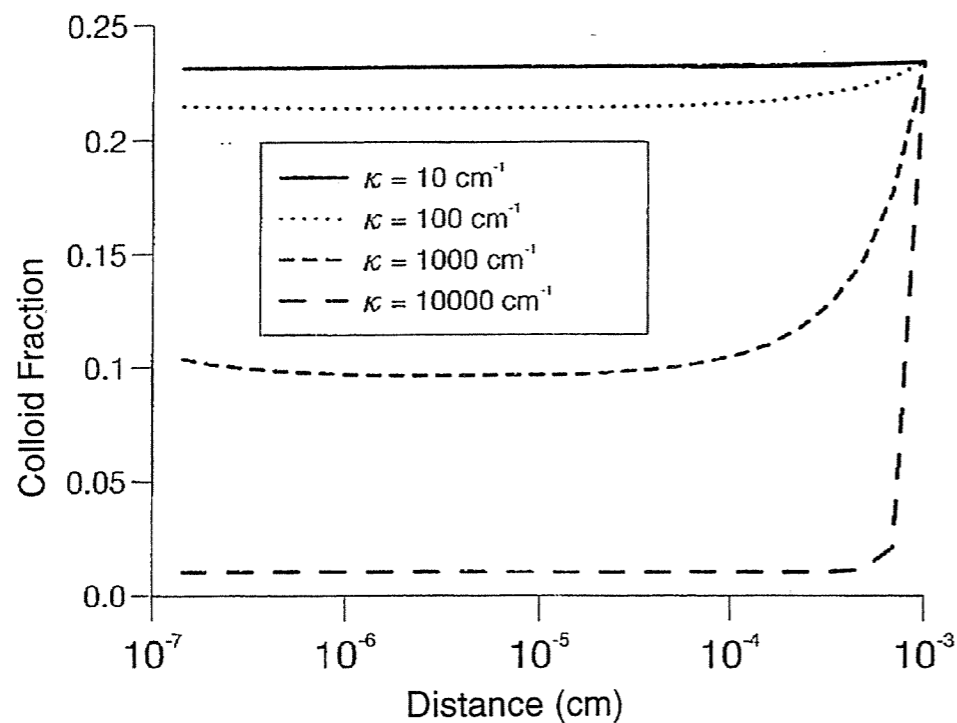
Figure 10   *Calculated colloid fraction as a function of distance from the grain core for a spherical grain of radius 10^{-3} cm, assuming a heterogeneous impurity distribution (see text). Dose rate 100 kGy/h, total dose 833 MGy.*
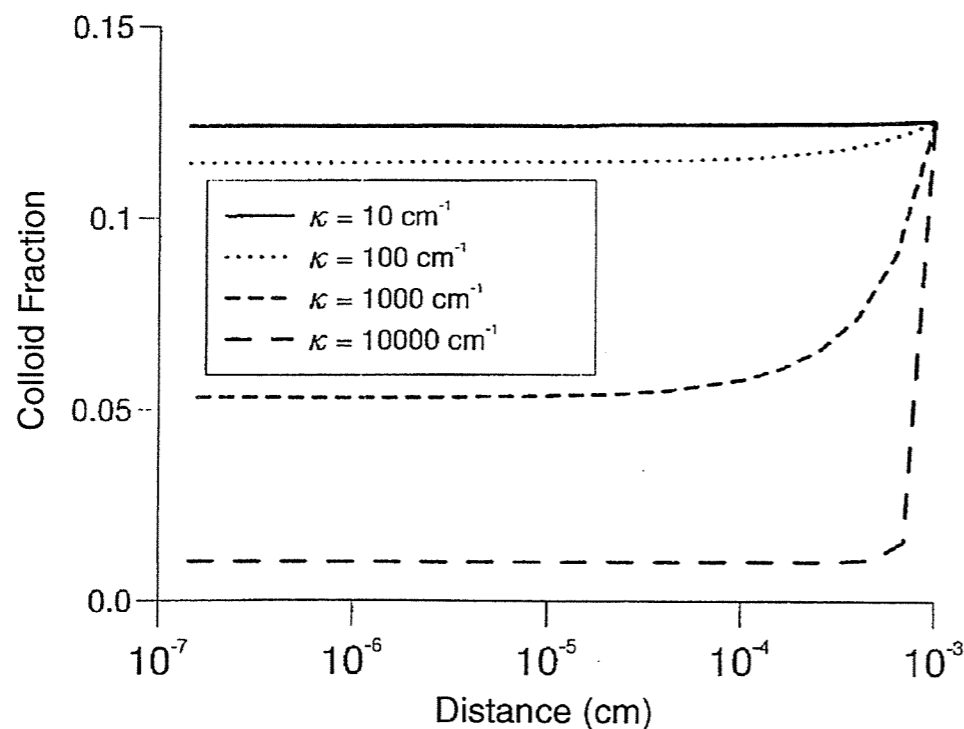

Figure 11   *Calculated colloid fraction as a function of distance from the grain core for a spherical grain of radius 10^{-3} cm, assuming a heterogeneous impurity distribution but disregarding the effect of diffusion (see text). Dose rate 100 kGy/h, total dose 833 MGy.*

$\kappa=10^3$ cm^{-1}, but further inspection of them learns that all curves have this same behaviour. The cause of this is that $\nabla^2 c_H$ is divergent for $r = 0$ because $c_S(0)$ is not equal to zero.

In Fig. 11 the results of simulations only differing from the previous in that they disregard the effect of diffusion have been presented. Two important differences with Fig. 10 can be observed in Fig. 11, first the colloidal fraction is systematically much lower (about a factor 2) than in Fig. 10; and second the U–form character of the curves has disappeared. We can see that the diffusion–term in this case is very important and cannot be disregarded.

6.   THE REPOSITORY.

On top of all the previously considered heterogeneities, there is as well an important gradient at the scale of a repository, e.g. the gradient resulting from the absorption of the gamma radiation by salt near the containers. This can be modelled as a gradient in the dose rate.
At the scale of the salt grains the dose rate gradient as a consequence of the sensitivity to "stopping rate" can be disregarded. However the question is whether the gradient which in a repository would develop radially away from the containers would significantly contribute to the diffusion . It is easy to observe that this is not the case. Lets assume that the dose rate can be described with:

$$K(d) = K_0 e^{-\kappa d} \qquad (16)$$

where d is the distance to the container. This leads to:

$$\nabla^2 c_F \propto \frac{1}{4}\kappa^2 c_F \quad \text{and}$$
$$\nabla^2 c_H \propto \kappa^2 c_H \qquad (17)$$

Now κ is of the order of magnitude of 1 cm^{-1} and $D_F c_F$ and $D_H c_H$ lie between 10^{-18} and 10^{-14} cm^2/s for $T \approx 100$ °C. If we now know that the dose rate of 10 kGy/h corresponds with

$$c_S(r) = c_{S,0}\, e^{-\kappa(R-r)} \qquad (12)$$

then, the zero order steady state equation for the H−centres is :

$$c_H = \frac{K}{K_2 c_F + z_H \rho_D D_H + D_H 4\pi r_C c_C + K_H c_S(r)} \qquad (13)$$

What gives (see equation (10)):

$$\nabla^2 c_H = -\frac{\kappa K D c_S(r)}{(C + D c_S(r))^2}\left[\frac{2}{r} + \kappa - \frac{2\kappa D c_S(r)}{C + D c_S(r)}\right] \qquad (14)$$

where $C = K_2 c_F + z_H \rho_d D_H + D_H 4\,\pi r_C C_C.$, and : $D = K_H.$

The first order steady state equation for the H−centres then becomes:

$$c_H = \frac{K + D_H \nabla^2 c_H}{K_2 c_F + z_H \rho_D D_H + D_H 4\pi r_C c_C + K_H c_S(r)} \qquad (15)$$

We were able to solve the "ordinary" equations for the F-centres (as determined by equations (2) and (3)), and for the colloids (as determined by equations (5) and (6)) in combination with these last expressed boundary conditions. The results for 4 values of κ are given in Fig. 10 for $c_{S,0} = 10^{-6}$, K equal to 100 kGy/h, and a total dose of 833 MGy. Firstly we can see that the colloidal fractions are in general higher than in the case considered for the dislocations, this is the effect of the impurities in general. For $\kappa = 10^4$ cm^{-1}, $c_S(r)$ is almost zero for $r = 0$ and we observe that the colloid fraction is also the same as that found for the dislocations. Moreover, it can be seen that the curves have an U shape (This can best be seen for

5. HETEROGENEOUS IMPURITY DISTRIBUTION

During crystal growth, lattice impurities tend to be preferently segregated towards the crystal exterior surfaces. Some crystals incorporate progressively higher concentrations of lattice impurities as they become bigger, and some times even stop growing due to "poisoning" of the growing surfaces by the impurities Moreover, in a closed system, a crystal growing from solution is bound to incorporate more and more impurities while growing (due to the changes in the solution concentration) until the exterior surface is "poisoned" and growth stops. In autigenic crystals, therefore it is logical to expect higher impurity concentrations near the crystal boundaries.

The impurity distribution in secondary crystals, which contrary to the autigenic have undergone some degree of recrystallization, can partially have controlled the mechanical behaviour of the crystal during the processes subsequent to crystallization. On the other side, the distribution of the impurities after a deformation process will be affected by deformation, e.g. impurities will partially redistribute themselves by diffusion towards the distended parts of the lattice which are dislocations and their arrangements.

Anyway, in rock forming minerals, impurities and dislocations have a tendency to fall near (and within) each other's sphere of influence, and to display gradients at grain and subgrain level.

Jain en Lidiard did not consider the effects of lattice impurities on the production of radiation damage. It can be assumed that certain impurities act as trapping environments for H centres and thus provoke an enhanced colloid growth. This assumption leads to an extra (negative) term in equation (5) : $K_H c_S c_H$ where c_S is the concentration of the impurities and K_H a reaction constant.

Lets assume, to ease our work, that the impurity concentration is stable and nonsaturable, we will therefore not consider the development of H−dimers.

Assuming that the space dependence for the impurities in an spherical grain is equal to that assumed for the dislocations so that:

$K = 1.667 \times 10^{-8}$ s^{-1} we can see that the contribution to diffusion is only relevant for very low dose rates (or for very high temperatures). Under these situations, indeed, no colloid growth can take place, and thus we could conclude that in general the diffusion contribution as consequence of a gradient in dose rate K can be disregarded as compared with the effect of K itself.

7.   CONCLUSIONS

With the implemented modifications the Jain–Lidiard model is capable of reproducing the observed microstructures for incipient colloid development. However, since the dynamics of the dislocations and impurities have not been modelled we are not yet able to explain why and how the colour distribution follows the creep structures.

8.   REFERENCES

H. DONKER and A. GARCÍA CELMA, 1995: *"Stored Energy in Irradiated Natural Rock Salt as Compared to Synthetic Halite of Different Characteristics"*, article 17 of this volume.

A. GARCÍA CELMA and H. DONKER, 1994: *"Radiation–Induced Creep of Confined NaCl"*, Rad. Eff. Def. Solids **132**, 223–247.

H. GIES, A. GARCÍA CELMA, J.B.M. DE HAAS, L. PEDERSON, T. ROTHFUCHS, 1994: *"Radiation Defects and Energy Storage in Natural Polycrystalline Rock Salt. Results of an In–situ Test in the Permian Rock Salt of the Asse"*, Mat.Res. Soc. Symp. Proc. **333**, 219–226

L.W. HOBBS, 1972: *"Transmission Electron Microscopy of Extended Defects in Alkali Halide Crystals"*, in "Surface and Defect Properties of Solids", Vol. 4, Specialst Periodical Reports, Ed. J.M. Thomas and M.W. Roberts (The Chemical Society, London), p. 152 – 250

L.W. HOBBS, 1976: *"Point Defect Stabilization in Ionic Crystals at High Defect Concentrations"*, J. Physique **37**, C7, 3–26

L.W. HOBBS, A.E. HUGHES and D. POOLEY, 1973: *"A Study of Interstitial Clusters in Irradiated Alkali Halides using Direct Electron Microscopy"*, Proc. R. Soc. Lond. **A332,** 167–185.

U. JAIN and A.B. LIDIARD, 1977: *"The Growth of Colloidal Centres in Irradiated Alkali Halides"*, Phil. Mag. **35**, 245–259.

J. SEINEN, J.C. GROOTE, J.R.W. WEERKAMP and H.W. DEN HARTOG, 1992: *"Radiation Damage in NaCl: General Model of Nucleation and Aggregation Processes in Doped NaCl"*, Rad. Eff. Def. Solids **124**, 325–339.

W.J. SOPPE, 1993: *"Computer Simulation of Radiation Damage in NaCl by using a Kinetic Rate Reaction Model"*, J. Phys.: Condensed Matter **5**, 3519–3540.

INTER AND INTRACRYSTALLINE CREEP PROCESSES OCCURRING DURING SALT IRRADIATION

A. García Celma and H. Donker

ABSTRACT

Results of the experiments performed by our group in the last eight years show that salt creeps due to irradiation provided the dose rate is low enough. This article summarizes the observations and arguments on which our conclusion is based.

Optical microscopy observation of salt samples before and after gamma-irradiation experiments was performed. The operation of radiation-induced intracrystalline creep processes was inferred from the presence in the irradiated samples of microstructures indicative of both incipient and very advanced creep which were not present in the unirradiated samples. The observations could be made by ordinary optical microscopy because dislocations in NaCl are decorated blue by the Na-metal colloids developed by irradiation. These intracrystalline creep microstructures were moreover observed to be coupled to radiation damage anneal at the microscopic level, and to contribute to the attainment of radiation damage steady state.

Intercrystalline creep processes were also proven to take place during irradiation. Amongst them the best observed was recrystallization because its operation annihilates all the crystal defects returning the NaCl to its original colourlessness. Recrystallization consumes the energy previously stored in the crystal defects. Two types of recrystallization were observed. One of them consists of the migration of new (and dry) grain boundaries created by intracrystalline creep. The other recrystallization type consists of the migration of already existing wet grain boundaries and is known as Fluid Assisted Recrystallization (FAR).

1. INTRODUCTION

Gamma-irradiation damages the NaCl crystals by developing lattice defects such as F- and H-centres. F-centres can precipitate forming Na-metal particles of colloidal size and properties. In order to develop colloids, a sufficient concentration of F-centres is necessary. A crystal containing F-centres and small quantities of colloidal sodium ($<10^{-5}$ molar fraction) becomes yellow. Higher amounts of colloidal sodium in the NaCl lattice turn the rock salt blue. The coloration of the salt therefore is related to the amount of damage, and thus observation of damage variations is possible by optical microscopy.

Three series of irradiation experiments were performed, all three at constant temperature (100°C) and at approximately constant dose rate (either 4 or 15 kGy/h), and each series up to ten different total doses between 0.02 and 45 MGy . Each experiment contained 16 different salt samples but different experiments of the same series had equivalent samples. These were the experiments called GIF B experiments which took place in the framework of the HAW-project. The methodology applied can be read in García Celma et al., [1995 a].

The samples consisted of natural rock salts, synthetic polycrystals and synthetic monocrystals. The natural rock salt samples were taken from the Asse Mine (Germany) and from the Potasas del Llobregat Mine (Spain). The synthetic polycrystals were prepared in the laboratory using as original material salt powder of analytic purity. The synthetic high purity single crystals were purchased from Harshaw Ltd. and were also poor in OH⁻ contents.

Equivalent samples were subject to equivalent irradiation experiments but differed from one another in that they could contain some added brine or not. Or they could have equal amounts of brine added but one of them was subjected to enhanced pressure (of 200 bar) during irradiation while the other was not.

This article reviews the observations made in thin sections of these samples and the interpretations made with the help of many other measurements and observations performed from 1986 on. We will first consider the links between the microstructures and the colloid development, and then the way in which intracrystalline creep anneals the radiation damage and will finish considering intercrystalline creep. Intercrystalline creep is in this case mostly "static"

recrystallization, since the samples were not subject to directional stress. More information on the same samples and experiments can be found in De las Cuevas and Miralles, [1995]; Donker and García Celma , [1995 a and b]; Donker et al., [1995] ; García Celma and Donker [1994 a and b]; and García Celma et al., [1993, and 1995 a and b]

2.   INCIPIENT   RADIATION   DAMAGE   DEVELOPMENT   AND MICROSTRUCTURES.

For the F-centres to precipitate and develop colloids in a NaCl crystal, they need to be kept from recombining with the H-centres. According to Hobbs et al., [1973] perfect edge dislocation loops (011) develop and coalesce in irradiated NaCl crystals. H-centres are fixed as Cl_2 molecules at both sides of the extra half plane of these loops, and thus kept from recombining with the F-centres. The F-centres on their side could precipitate in the dislocation lines as suggested by Hobbs [1976].

García Celma and Donker, [1994 b] show that, since dislocation structures are mostly blue (colloid containing) and they constitute creep microstructures which were not present before irradiation, colloids do not only develop together with the dislocations and at the dislocation lines, but migrate and anneal together with them.

However, even if complementary defects are fixed at different crystallographic sites regarding a given crystallographic direction, nucleation of defect aggregates such as colloids would be greatly improved if a field of diffusion would be imposed to the homogenous crystal. This field can be created by the existence of important sinks such as dislocation walls ((sub)grain boundaries).

For all the irradiated samples microstructural observation shows that the first colloid development takes place at the grain boundary region. The portion of the crystal in contact with the exterior surface is devoid of colloids and constitutes a white band of variable thickness (2 to 7 μm) which is limited inside the crystal by a dark blue line parallel to the crystal boundary. In crystals with incipient colloid development, from this dark blue line towards the centre of the crystal the blue colour gradually fades out. Levy et al., [1980] observed the white rims at the

grain boundaries of irradiated salt samples and showed them to be coupled to a higher content of impurities. They interpreted these rims as due to difficulties of colloid nucleation caused by impurities. Figures 1 and 2 show the aspect of these microstructures, see as well García Celma and Donker, [1994 a and b] and García Celma et al., [1995 b] for other appearances of the same microstructure.

This microstructure presents the same characteristics as the void distribution in irradiated metals described by Bullough and Nelson, [1974]. Bullough and Nelson, [1974] show that, in the area of the crystal boundaries, voids are absent at the exterior surface, while at a short distance within the crystal a sharp line parallel to the exterior surface marks an area of a very high void concentration behind which, towards the interior of the crystal, the void concentration gradually diminishes. This distribution would be reached thanks to the creep mechanism described by Nabarro, [1948] who observed that irradiation produces deformation of metals, and proposed a mechanism consisting of preferential diffusion of vacancies and interstitials, produced by irradiation, towards crystal boundaries, where they disappear. This diffusion would create a concentration gradient and therefore a stress field would develop which could drive crystal defects.

Jiménez de Castro and Álvarez Rivas, [1990] show that most of the stored energy produced by irradiation of NaCl is found at the surface of the crystal.

On the basis of the microstructural observations of the white-blue boundaries García Celma et al., [1995 b] developed a version of the Jain Lidiard model with a description of the dislocation density gradient to be expected at a grain boundary and a definition of the grain boundary itself in terms of dislocation density and calculated the colloid density as a function of the distance to the grain boundary. They found a distribution of colloids equivalent to that of the voids in Bullough and Nelson, [1974] and to that of the colloids found in the microstructure reproduced in Figures 1 and 2.

Therefore the existence of crystal exterior surfaces (or of the grain boundaries) could be important for the stabilization of radiation damage. The existence of material discontinuities functioning as huge sinks for crystal defects combined with the effect of the different diffusivities towards them create gradients of defect concentration which make the precipitation
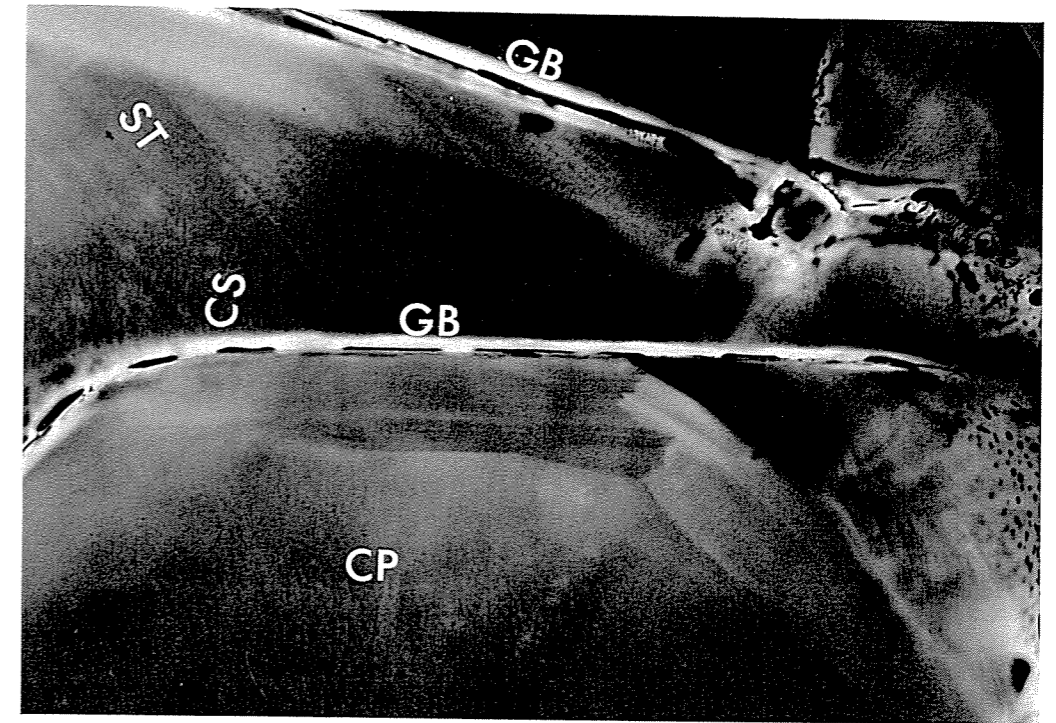
Figure 1 :   *Colourless bands at grain boundaries (GB). Slip traces (ST) cross slip (CS) structures and cellular patters (CP) indicated.   See as well Fig.4. Asse Speisesalz sample, 15 Sp-800. Irrad. cond.: 100°C, 4 kGy/h, 4.6 MGy. Mag. 216 X*
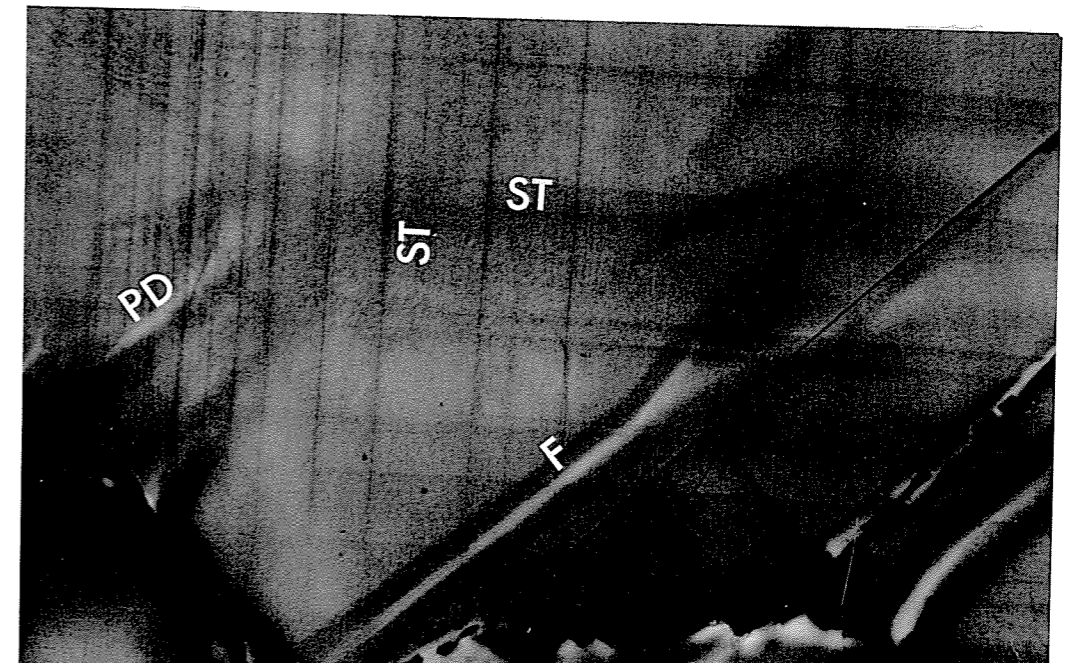

Figure 2.   *Colourless rims limited by intense blue lines developed at (001) fractures (F) and also at plastic deformation (PD) structures. Slip traces (ST) <011> indicated. Asse Speisesalz sample T1 Sp-800. Irrad. cond.: 100°C, 15 kGy/h, 2.6 MGy . Mag. 338 X.*

of different defects in different areas of the crystal possible. At the lattice level, of course, the defects would precipitate in their corresponding places, with the difference that the possibility to reach their sites before recombining is greatly improved by the existence of a gradient which acts differently on the different defects (due to their different diffusivities).

3. INTRACRYSTALLINE CREEP AND DEVELOPMENT OF RADIATION DAMAGE STEADY STATE (SATURATION).

First we will summarize a couple of creep principles. As long as most dislocations can move, the stress within a crystal lattice can be resolved in a plastic way, and the crystal creeps. Dislocation motion brings dislocations together. Negative interferences annihilate the dislocation, repairing the crystal lattice. Positive interferences produce rearrangements in lower energy structures such as dislocation walls [Hull and Bacon, 1984]. Dislocation walls, due to the preferential diffusion along them, produce a gradient of defect concentration which forces diffusion towards these walls. Thus impurities are forced towards grain and subgrain boundaries where also the highest dislocation wall density is present.[Sabharwal et al.,1975; Harris and Fiasson, 1976; Geguzin et al., 1976; Riggs and Wuttig, 1969; Filippov and Gaidukov, 1993]

Hobbs [1976] observed that the perfect edge dislocation loops which develop by irradiation in ionic crystals, grow and coalesce and give rise to dislocation forest development. Dislocation forests are considered to be the reason of hardening in crystals, because in dislocation forest the dislocations pin each other hindering each others mobility and thus the plastic behaviour of the material. They are the reason of the hardening undergone by NaCl when irradiated. Dislocation forests cannot be observed in salt by optical microscopy.

Senseny et al., [1992] gave a list of the substructural processes taking place under increasing total strain for rock salt and of the microstructures thus produced and related them to the three stages of a creep curve. This was summarized by García Celma and Donker [1994 b] as shown in Fig. 3. The hardening stage (stage I) corresponds to the development of dislocation forest development. Where the creep curve bends to enter stage II, glide is active. In stage II cross slip is added to glide, and at the end climb can take place. Rotation

388

recrystallization is added to the rest of the processes in the accelerated creep part, stage III. All this under the assumption that temperature and confining pressure are high enough and strain rate low enough to allow plastic behaviour of the rock.
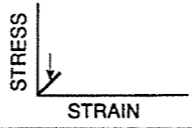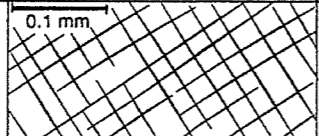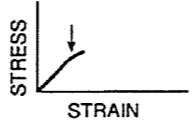
All the microstructures here described are diagnostic of different dislocation motion mechanisms and have been observed after chemical etching of deformed NaCl [Urai et al. 1987]; in aditively coloured samples they are decorated by colloids as well [Amelinckx, 1964].

Dry (sub)grain boundaries are generally present in the non irradiated Asse Speisesalz samples, and cellular patterns could have been in some crystals or some of the Asse samples, but the slip traces of Fig. 4, the subgrains in Fig. 5, and the new grains of Fig. 6 certainly develop during irradiation of Asse Speisesalz and of Harshaw single crystals which did not have any of these structures before irradiation.

The (blue) deformation structures which were not present in the original material are the microstructural expression of incipient creep (slip traces, Fig. 4) and final creep (foam texture) (Fig. 6) [Senseny et al., 1992]. Therefore it has to be concluded that dislocation motion occurred during irradiation. Moreover, there are many crystals which show intermediate structures (Fig. 5), suggesting change from one creep mechanism to another, and although we have to recur to the deformation literature to know which microstructure is transforming into which [Senseny et al., 1992] (Fig. 3), it cannot be doubted that the samples crept during irradiation and that this creep kept them from further hardening under the influence of the gamma-radiation.

The observed dislocation arrangements are in all stages colloid-decorated. Therefore the sodium colloids have to have migrated during irradiation tracking the deformation structures. Probably a dislocation line cannot drag along a big colloid. It seems reasonable to assume that colloids are annealed from some places and re-developed in others, e.g. are eliminated from places where dislocations went through (from the cores of the developing (sub)grains). This means that an anneal mechanism of radiation damage defects, which is different from that usually considered in the theoretical models, has to be taken into account. It also means that the rate controlling mechanisms of this anneal are the rock creep mechanisms.

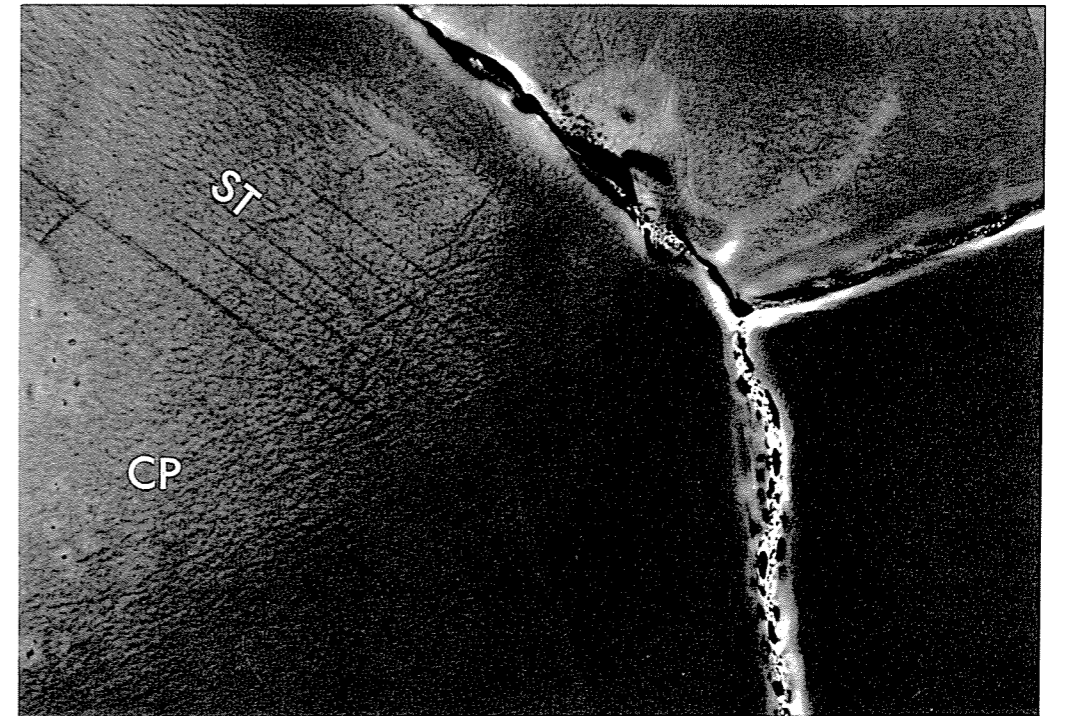| DISLOCATION MOTION MECHANISM	DIAGNOSTIC MICROSTRUCTURE		ONSET OF MECHANISM AND ITS EFFECT ON "A CREEP CURVE"
	MORPHOLOGY	NAME	
DISLOCATION DEVELOPMENT	NOT VISIBLE IN OPTICAL MICROSCOPY	DISLOCATION (FORESTS)	
GLIDE		SLIP TRACES	
CROSS SLIP		CRENULLATED SLIP TRACES	
		WAVY SLIP	
		CELLULAR PATTERNS	
CLIMB		SUBGRAINS (POLYGONS)	
DISLOCATION WALL MIGRATION		FOAM-TEXTURE	

Figure 3.   *The diagnostic creep microstructures and the mechanisms of dislocation rearrangement which produce them. GB stands for grain boundary, B for brine, and SGB for subgrain boundary. Reproduced from Garcia Celma and Donker, [1994 b]. Based on Senseny et al., [1992].*

Figure 4.   *Slip traces (ST), to cross slip and cellular patters (see as well Fig.3).*
Colourless grain boundary with black structures. Asse Speisesalz (15 Sp800).
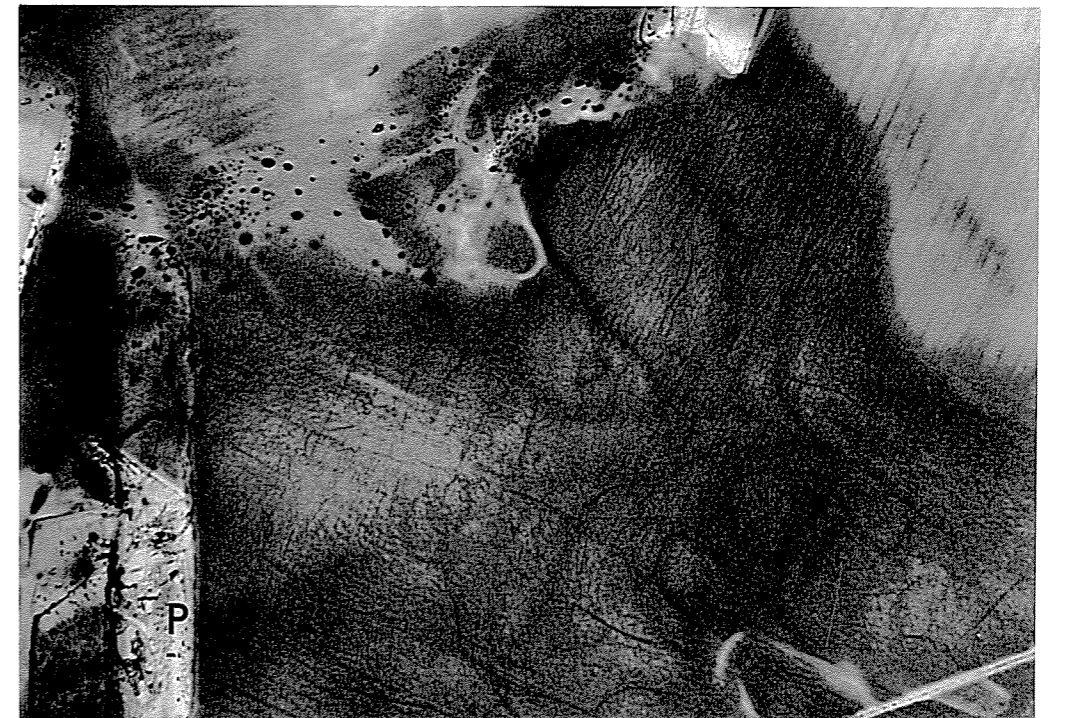*Irrad. cond.: 100°C, 4 kGy/h and 4.6 MGy. Mag. 216 X.*

Figure 5.   *Subgrain boundaries developing from rearrangement of cellular patterns. The*
grain boundary between the polyhalite (P) and the halite contained many fluid
inclusions, the black structures. Asse Speisesalz (T3 Sp800). Irrad. cond.:
100°C, 15 kGy/h, 4 MGy. Mag. 216 X.

García Celma and Donker [1994 a] observed that anneal associated to creep structures is more active in natural rocks than in pure undeformed single crystals. Since the samples on which this statement was based were irradiated simultaneously, the reasons for this must lie in the differences between the samples; either intracrystalline enhancement of creep by H_2O (dislocation mobility enhancement by H_2O) [Carter and Hansen, 1983] is very important, or polycrystallinity is. Most probably both.

Regarding the enhancement of dislocation mobility by H_2O it can be seen that around polyhalites, at which boundary with halite many fluid inclusions are present before irradiation, a blue aureole develops for low total doses while the most intense recovery processes (see Fig.6) are observed for high doses. On the other hand, the competence contrast between polyhalite and halite could also cause deformation structures to develop at their boundaries by partitioning of the otherwise homogeneous stress field to which the samples are subject during irradiation. These homogeneous stresses must then be the result of confined thermal expansion of the samples since the experiments take place at 100°C and all microstructures appear in the samples regardless of whether they were subject to enhanced pressure during irradiation or not.

Two reasons can be suggested to explain the enhancement of anneal associated to creep during irradiation in polycrystals as compared to our single crystals: grain size differences between the considered samples and grain shape interferences when volume changes are required.

The influence of grain size is due to the fact that the volume of preferred diffusion paths is important in damage development and creep. This volume is much higher in the natural rocks than in the single crystals. The single crystals used in the experiments consist of tablets with a diameter of 24.28 mm and a length of 10 mm, and without subgrains. In Sp-800 samples the individual crystals can be approximated by spheres with a mean diameter of 5 mm which moreover include a web of subgrains of a diameter of about 200 micron. Preferred diffusion and sinking of lattice defects towards dislocation arrangements in grain and subgrain boundaries has to be more important in Sp-800 samples than in the pure single crystals. This could produce differential stresses within the crystals [Nabarro, 1948] which would enhance dislocation mobility.

Let us consider the shape interferences. When a grain becomes larger the neighbouring grains will have to accommodate their shapes to this expansion. In our case, volume increase due to dislocation loop development and accommodation of the Cl_2 molecules and to thermal dilation (because of the 100°C at which the experiments were performed) has to be expected. Thanks to different intensities of slip and/or climb of dislocations in the different crystallographic planes, the crystal shape can change when placed under differential stress by an expanding neighbour. The differential stress is produced by partitioning of deformation depending on the relative crystal exterior shapes, e.g. if the boundary between two crystals displays a sharp angle and one of the crystal expands more in this direction because (e.g.) it contains more impurities (which ease dislocation loop nucleation), then the homogeneous stress field is partitioned into differential stresses and dislocation migration (or crack development) takes place. It is therefore easier for colloids to interfere with passing dislocations than would be the case when the slip planes are only determined by irradiation-produced dislocation loops mobility, as in the single crystals.

Regarding the intracrystalline processes taking place during irradiation of polycrystals it is important to take into account that at the start of a deformation episode different grains can be in different states of strain, that strain is higher at grain mantles since by developing dislocations in the mantles the cores of the grains are protected from deformation, and that depending on the orientation of each grain with respect to the deformation the rate of each process will be different in each grain. Thus one grain can display advanced recovery structures while another may start to develop damage microstructures.

We assume that the fact that the stored energy accumulated in lattice defects saturates for natural samples at values lower than that corresponding to colloid saturation as calculated using the Jain-Lidiard model for the corresponding experiment is due to the operation of creep processes [Donker and García Celma, 1995 a]. The experiment in which saturation of damage was reached was such that fluid assisted recrystallization had to be excluded of the possible reason for the low stored energy values. Note then that the low value of stored energy at saturation could be due not only to the development of a possible creep steady state and therefore stabilization of stored energy attached to dislocations, but also to the enhanced anneal of the rest of radiation damage defects which crept together with the dislocations [Donker and García Celma, 1995 a].
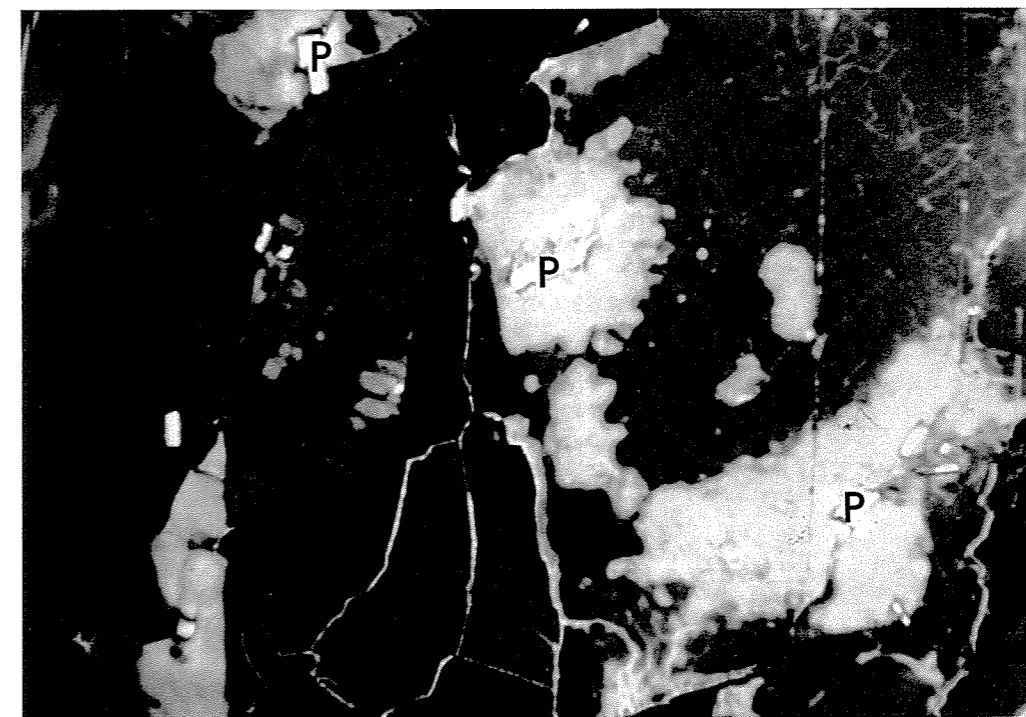
Figure 6 a.   *Anneal of colloids produced by dislocation wall migration ("dry" recrystallization). Note however, that these bleached areas can contain polyhalite (P). Asse Speisesalz (T41 Sp-800). Irrad. cond.: 100°C, 15 kGy/h , 15.9 MGy. Mag. 34 X*
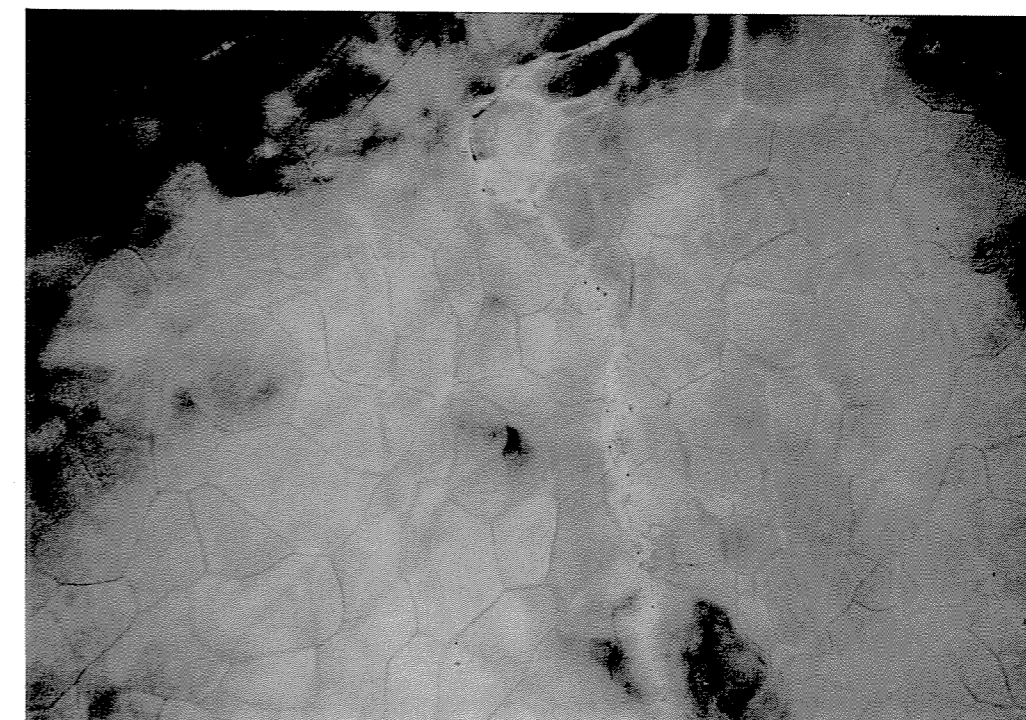

Figure 6 b.   *Foam texture developed by dislocation wall migration ("dry" recrystallization) inside the bleached areas observed in Fig. 6 a. Asse Speisesalz (T50 Sp-800). Irrad. cond. : 100 °C, 15 kGy/h , 15.9 MGy. Mag. 134 X.*

Taking into account the properties of creep [Guillope and Poirier, 1979; Poirier, 1976], this additionally means that, at least if the irradiated samples are not allowed to expand during irradiation, lower irradiation dose rates (deformation rates) enhance recovery and the associated anneal versus damage development. Saturation of radiation damage (steady state) would be reached at lower levels of damage for lower dose rates in polycrystalline samples.

## 4. INTERCRYSTALLINE CREEP PROCESSES (RECRYSTALLIZATION) AND RADIATION DAMAGE ANNEAL.

The only intercrystalline processes which have been observed in the samples being considered are recrystallization processes. First of all, the well known "dry" recovery recrystallization, which takes place as a consequence of the creep processes described above, and then an additional type of recrystallization, which depends on the existence of brine at the grain boundaries and which is called Fluid Assisted Recrystallization (FAR).

The "dry" recrystallization is a consequence of the development of dislocation walls which result of the combined action of glide and climb inside a crystal. With increasing deformation (radiation-induced in our case) the misorientation between parts of a crystal across the dislocation walls becomes so important that the dislocation walls acquire the properties of grain boundaries and try to reduce their surface energy. This is reached by migration until the grain boundaries become straight and meet at triple points delineating angles of 120 degrees, what constitutes the characteristic high equilibrium "foam" texture (see figure 3). Wherever a foam texture is found it has to be assumed that grain boundary migration (recrystallization) took place. Note that recrystallization always implies that, the material which constituted the old crystal (which is being invaded by the migrating grain boundary) is incorporated step by step in the lattice of the new grain, but the lattice defects of the old crystal are not (except for perhaps some impurities). In this way the previous defects are annealed and the structure is recovered [Guillope and Poirier, 1979; Senseny et al., 1992]. This has been the case in the structure of figure 6.

Fluid Assisted Recrystallization (FAR) on the contrary consists of "wet" grain boundary migration. A "wet" grain boundary can be observed in Fig. 7. FAR proceeds by solution of

damaged NaCl in the brine at the grain boundary voids, transport in solution, and reprecipitation of newly produced NaCl. In this way the wet grain boundary migrates [Urai et al., 1986; Urai, 1983]. Note that this process also eliminates the defects which were present in the old crystal, since it is dissolved in the brine.

García Celma et al., [1988] showed that FAR extensively takes place (after irradiation) in heavily irradiated samples and eliminates radiation damage. In their experiments FAR operation was proven by the existence of fluid inclusions containing H_2 and decorating the growth surfaces of the recrystallized grains. Hydrogen is produced by the reaction:

$$2 \, Na + 2 \, H_2O \rightarrow 2 \, NaOH + H_2$$
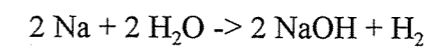
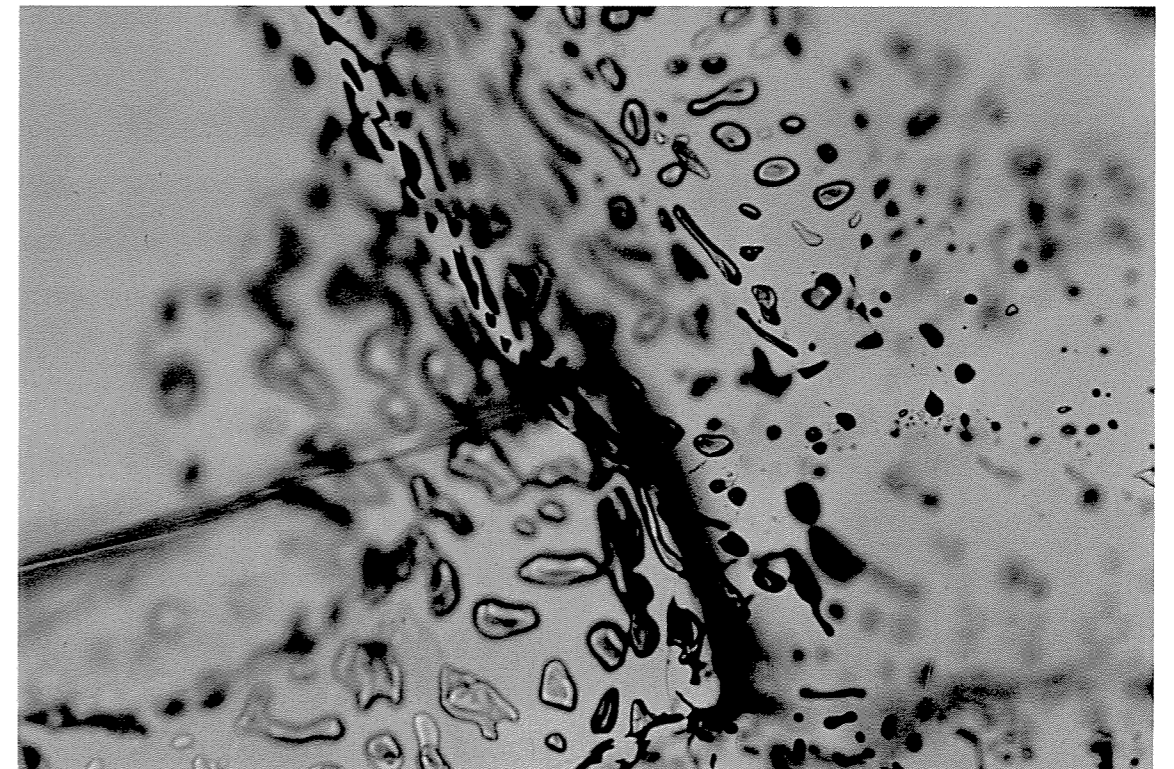which takes place during solution of the Na-colloids at the grain boundary void.

Figure 7: *Wet grain boundary. The voids in the grain boundary surface at various depths contain brine or have lost it during section preparation in which case they are observed as black. Micrograph of a "thick" thin section of an Asse Speisesalz sample (8Sp-800) . Mag. 216 X*

Characteristic of FAR-produced areas is that their contacts with the blue material are, on one side a wet grain boundary, and on the other side the previous position of the grain boundary. FAR-produced areas present the morphology of overgrowths. Moreover, FAR-produced areas have different substructures (e.g. subgrain boundaries) than the rest of the crystal, and are perfectly white (see Fig. 8), except when re-irradiated (see Fig.9).

Whether Fluid Assisted Recrystallization could proceed without decomposing brine and/or with brine in the vapour phase was a matter of discussion. If recrystallization can proceed without decomposing brine and can also proceed when the brine is in the vapour phase, can proceed during irradiation and cyclically, then recrystallization could operate continuously in a repository. These questions were solved by García Celma et al., [1993]. They showed that the solution of irradiated NaCl in H_2O, which is the process responsible for brine decomposition during FAR, only decomposes the H_2O when the F-centres have precipitated as Na-colloids. Therefore, as long as colloids have not developed, FAR can proceed while the amount of brine at the grain boundary is maintained. García Celma et al., [1993] also proved that solution and reprecipitation of NaCl, which is per definition FAR, takes place at 150°C and atmospheric pressure, in which conditions brine has to be in a vapour state. Their proof was that grain growth takes place in samples subject 150°C and atmospheric pressure. Therefore, FAR can take place even if the brine is in the vapour phase. Since samples not subjected to these temperatures did not recrystallize, the enhancement of FAR by temperature was proven.

The occurrence of FAR during irradiation was also proven by García Celma et al., [1993] since, in order to produce variations in grain sizes, the grain boundaries have to migrate and grain boundary migration is per definition recrystallization and they showed grain growth to take place during irradiation (compare Fig. 10 with Fig. 11). To explain their quantitative microstructural determinations they also had to assume that recrystallization took place more than twice on the same material during the experiments. These experiments had been performed with samples consisting of cold pressed NaCl powder of a starting microstructure as shown in Fig. 10 and an end microstructure as that of Fig 11. These recrystallization was enhanced by brine; and thus inferred to be FAR.
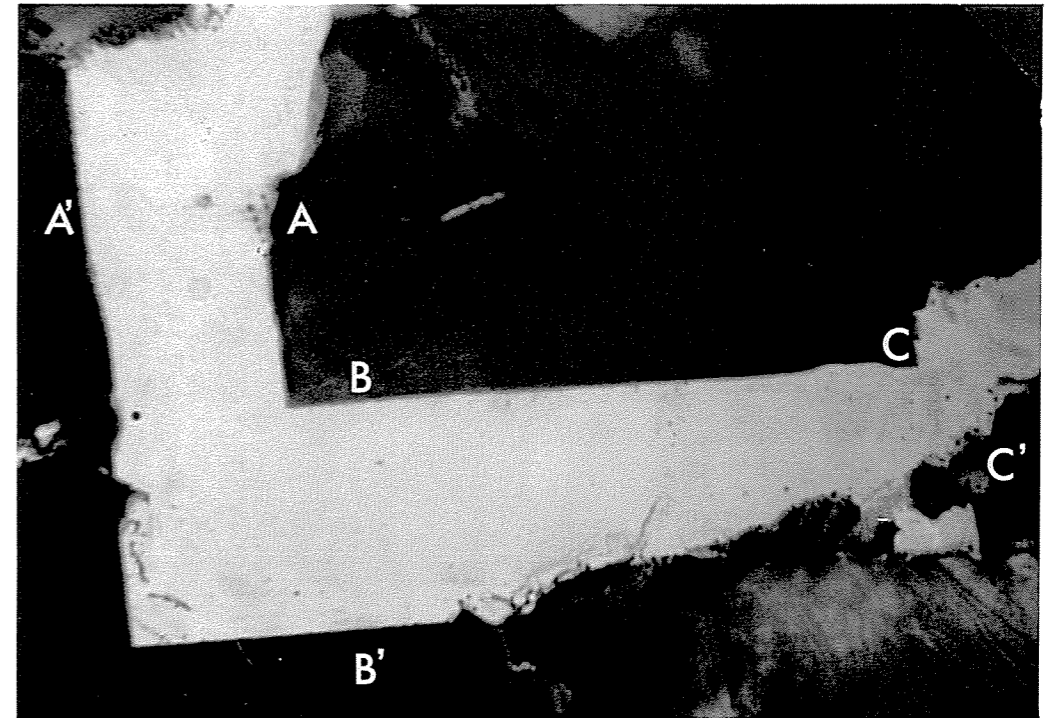
Figure 8 a : *Fluid Assisted Recrystallization. The grain boundary at ABC has migrated to A'B'C' and the colloids have been completely annealed. Asse Speisesalz sample T8 Sp-800. Irrad. cond: 100°C, 15 kGy/h, 7 MGy. Mag. 86 X.*
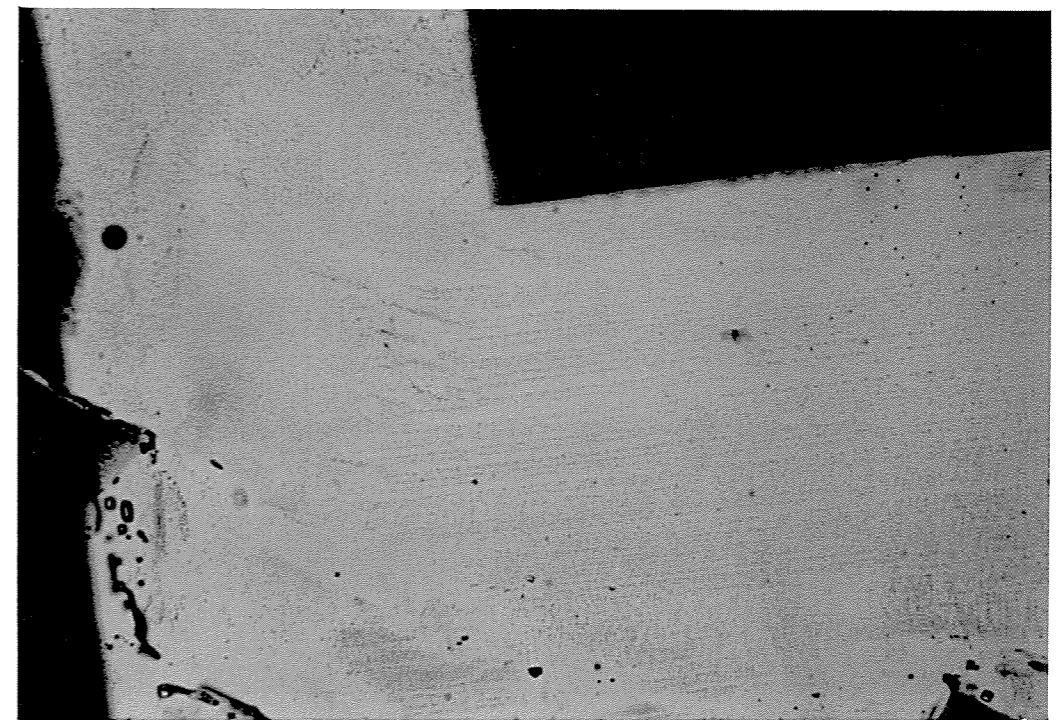

Figure 8 b: *Blow up of Fig. 8 a. Little bubbles arranged in lines consist of fluid inclusions characteristically containing H_2 originating from the reaction of the Na-colloids with brine which is incorporated in the growing surfaces. Mag. 216 X*
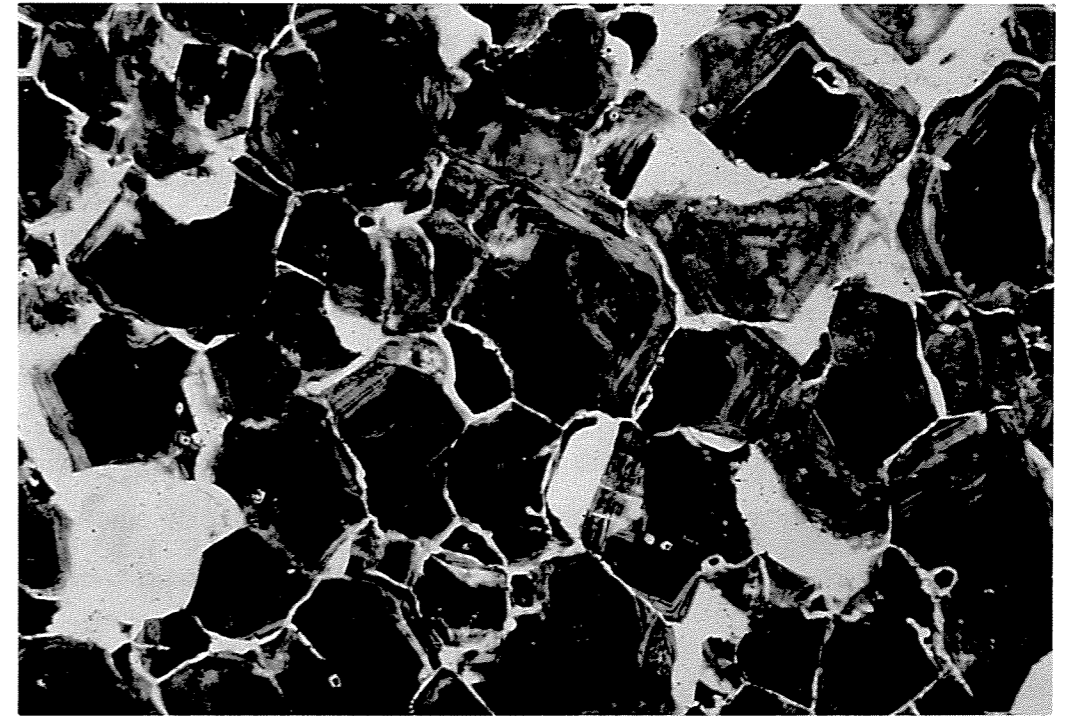
Figure 9: *Characteristic aspect of FAR grown and redecorated grains. Compare the size of the grains with that from Fig.10. NaCl Pressed Powder sample (20PP). Irrad. cond. : 100°C, 15 kGy/h, 44.6 MGy. Mag. 97 X.*
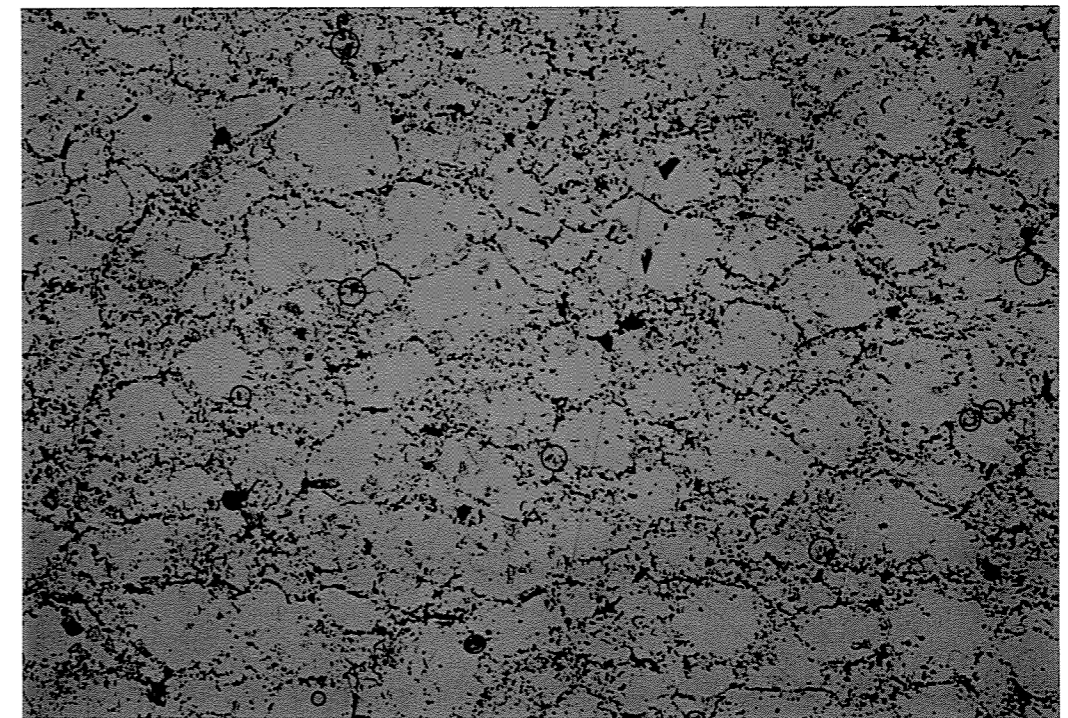

Figure 10: *Micrograph of the original structure of the NaCl Pressed Powder samples before irradiation. Compare with Fig 9 to see the difference in grain size. Same magnification as Fig.9. Mag. 97 X.*

5. INTERPRETATIONS AND PARTIAL CONCLUSIONS

At a low dose rate (15 kGy/h) and a high temperature (100°C), and in samples not allowed to dilate, mechanical distortion produced by irradiation leads to the development of plastic deformation (creep) structures, even in the absence of an externally applied differential stress. This effect is more important in polycrystals than in monocrystals.

At 15 kGy/h and 100°C the sodium colloids produced by irradiation migrate together with the deformation structures, and are therefore either dragged by the migrating dislocation, or annealed from some places and redeveloped at others, while creep proceeds. The actual process at atomic level is not yet understood.

Anneal coupled to intracrystalline creep processes can justify that the most damaged parts of natural crystals do not contain more stored energy than pure single crystals, at least when irradiation proceeds at a dose rate of 15 kGy/h, at a temperature of 100°C and when the samples are not allowed to dilate.

For high total doses (from 12 MGy on), obtained at a dose rate of 15 kGy/h, a temperature of 100°C, and in samples not allowed to dilate, climb of dislocations leading to recrystallization competes with fluid-assisted recrystallization in eliminating radiation damage. This recrystallization could have been influenced by the presence of OH$^-$ as lattice impurity, but is due to irradiation. An intragranular mechanism implying water-enhanced dislocation mobility could have been active but whether H$_2$O diffusion plays a major role in anneal of colour centres cannot be quantitatively determined. Note that diffusion of radiation damage defects towards (sub)boundaries can produce the same microstructures and we have not found any quantitative relationship between intragranular bleached areas an water content.

These creep processes show that the behaviour of the rock salt during irradiation is plastic, and suggested that a sort of steady state of radiation damage could be reached if the distorting agent (the radiation) was applied slowly enough (low dose rate) and during long enough times so as to already have produced damage enough (high total doses) for recovery to proceed. Although in themselves these microstructures do not prove that this steady state

would exist, their observation drove us to perform very long experiments which did prove that saturation of radiation damage exists for natural rock salts. This means that at lower dose rates, lower values of damage at saturation ought to be found. The radiation damage simulation models also reproduce saturation behaviour [see Donker and García Celma, 1995 a] and the lower values obtained in the experiment as compared to the predictions can be justified by the bleaching associated to creep.

6. GENERAL CONCLUSIONS

The intracrystalline microstructure analyses thus have shown that crystals creep during irradiation and in this way anneal some of the produced radiation damage. On the other hand, the analyses also have shown that nucleation of defect aggregates is easied by the existence of heterogeneities mostly bound to grain boundaries. Impurities, although spatially linked to colloid depleted areas, do not hinder damage development but, are segregated to the places [(sub)grain boundaries] where, due to enhanced diffusion, anneal of colour centres and dislocations takes place. Therefore the white-blue rims at the grain boundaries are not the consequence of hindered colloid nucleation but of differential diffusion. These rims, when unequally developed ought to be the reason for the nucleation of the first bulge for fluid assisted recrystallization.

Fluid-assisted recrystallization already takes place at intergranular brine contents of 0.02 weight %, can take place during irradiation and does not decompose the intergranular brine as long as colloids have not yet developed, can also take place if the brine is in the vapour phase and continues to take place even when the whole sample has already been recrystallized.

It will depend on the rate of volumetric recrystallization and that of colloid development whether brine will or will not be decomposed by recrystallization in a repository. The relative rates of colloid development and volumetric recrystallization deserve more attention.

REFERENCES

S. AMELINCKX, 1964 : *"The Direct Observation of Dislocations"*. Solid State Physics, Vol. **6** , Academic press, New York and London, 487 pp.

R. BULLOUGH and R. S. NELSON, 1974 : *"Voids in Irradiated metals"*. Phys. Tech. **5** : 29-67.

N. L. CARTER and F. D. HANSEN, 1983 : *"Creep of Rock Salt"* . Tectonophysics. **92**: 275-333

C. DE LAS CUEVAS and L. MIRALLES, 1995 : *"Colour Centres Development by Gamma-Irradiation of Natural and Synthetic Rock Salt Samples"*. Article Nr. 15, this volume.

H. DONKER and A. GARCÍA CELMA , 1995 a : *"On the Saturation of Radiation Damage in Natural Rock Salts"*. Article Nr. 18 this volume.

H. DONKER and A. GARCÍA CELMA , 1995 b : *"Stored Energy in Irradiated Natural Rock Salt as Compared to Synthetic Halite of Different Characteristics"*. Article Nr. 17, this volume.

H. DONKER , W. SOPPE and A. GARCÍA CELMA , 1995 : *"On the Relationships between Stored Energy and Colloidal Sodium Production in Irradiated Rock Salt"*. Article Nr. 19 this volume.

A. P. FILIPPOV and G. N. GAIDUKOV, 1993 : *" Formation of Impurity Segregation in the Field of Electric Stresses Near Dislocations"*. Phil. Mag. **A67** : 109-125.

A. GARCÍA CELMA and H. DONKER, 1994 a : *"Stored Energy in Irradiated Salt Samples"*. Commission of the European Communities. Nuclear Science and Technology Series. Topical Report, Nr. EUR 14845 EN, Luxembourg 127 pp.

A. GARCÍA CELMA and H. DONKER, 1994 b : *"Radiation- induced Creep of Confined NaCl "*. Rad. Eff. and Def. in Sol. **132** : 223-247.

A. GARCÍA CELMA, J. L. URAI, C. J. SPIERS 1988 : *"A Laboratory Investigation into the Interaction of Recrystallization and Radiation Damage Effects in Polycrystalline Salt Rocks"*. Commission of the European Communities. Nuclear Science and Technology Series, EUR 11849 EN, Luxembourg 125 pp.

A. GARCÍA CELMA, C. DE LAS CUEVAS, P. TEIXIDOR, L. MIRALLES and H. DONKER, 1993 : *"On the Possible Continuous Operation of an Intergranular Process of Radiation Damage Anneal in Rock Salt Repositories"*. In: Geological Disposal of Spent Fuel and High Level and Alpha Bearing Wastes, Proceedings of a Symposium, Antwerp, Belgium, 18-23 October 1992 . International Atomic Energy Agency, Vienna, 1993, p 133-144.

A. GARCÍA CELMA, A. J. NOLTEN, W. A. FELIKS, and H. VAN WEES, 1995 a: *"Gamma Irradiation Experiments in Natural and Synthetic Halite"*. Article Nr.6 this volume.

A. GARCÍA CELMA , W. SOPPE and H. DONKER, 1995 b : *"The Effect of Crystal Defect Density Gradients on Radiation Damage Development and Anneal"*. Article Nr. 20 this volume.

YA. GEGUZIN, E. R. DOBROVINSKAYA, I. E. LEV and M. V. MOZHAROV, 1967 : *"Cation Diffusion along the Boundaries in Alkali-Halide Bicrystals"*. Sov. Phys. Sol. State **8**, 2599-2603 .

M. GUILLOPE and J. P. POIRIER, 1979 : *"Dynamic Recrystallization During Creep of Single-Crystalline Halite: and Experimental Study"*. J. Geophys. Res. **84** : 5557-5567

L. B. HARRIS and J. FIASSON, 1976 : *"Cation Diffusion along Boundaries in Sodium Chloride"*. Phys. Stat. Sol. (a) **33** : 697-706.

L. W. HOBBS, 1976: *"Point Defect Stabilization in Ionic Crystals at High Defect Concentration"* Journal de Phys. **37**, Colloque C7: 3- 26.

L. B. HOBBS, A. E. HUGHES and D. POOLEY, 1973: *" A Study of Interstitial Clusters in Irradiated Alkali Halides Using Direct Electron Microscopy"*. Proc. R. Soc. Lond. **A332** : 167-185.

D. HULL and D. J. BACON, 1984 : *"Introduction to Dislocations. International Series on Materials Science and Technology"*. Vol. 37 . Pergamon Press, Oxford, 256 pp.

U. JAIN and A. B. LIDIARD, 1977 : *"The Growth of Colloidal Centres in Irradiated Alkali Halides"*. Phil. Mag. **35**: 245-259.

M. JIMÉNEZ DE CASTRO and J. L. ÁLVAREZ RIVAS, [1990]: *"The Surface Effect on the Stored Energy in Gamma-Irradiated NaCl and LiF"*. J. Phys.: Condens. Matter **2**; 1015-1019.

P. W. LEVY, K. J. SWYLER and R. W. KLAFFKY, 1980 : *"Radiation Induced Colour Center and Colloid Formation in Synthetic NaCl and Natural Rock Salt"*. J. de Phys. **7** (C6) : 344-347.

F. R. N. NABARRO, 1948 : *"Deformation of Crystals by the Motion of Single Ions, Report of a Conference on Strength of Solids (7-9 July 1947)* ". The Physical Society, London.

J. P. POIRIER 1976 : *"Creep of Crystals (High-Temperature Deformation Processes in Metals, Ceramics and Minerals)"*. Cambridge Earth Sciences Series, Cambridge University Press, U. K. 260 pp.

K. R. RIGGS and M. WUTTIG, 1969 : *"Cation Grain Boundary diffusion in Sodium Chloride"* . J. Appl. Phys. **40** : 4682 -4683.

K. S. SABHARWAL, J. MIMKES and M. WUTTIG, 1975: *"Anion Grain Boundary Diffusion in Sodium Chloride"* J. Appl. Phys. **46** : 1839-1840.

P. E. SENSENY, F. D. HANSEN, J. E. RUSSELL, N. L. CARTER and J. W. HANDIN, 1992 : *"Mechanical Behaviour of Rock Salt : Phenomenology and Micromechanics"*. Int. J. Rock. Mech. Min. Sci. & Geomech. Abstr. **29** : 363-378.

J. L. URAI, 1983 : *"Deformation of Wet Salt Rocks"*. Ph.D Thesis, Utrecht University, the Netherlands, 221 pp.

J. L. URAI, W. D. MEANS and G. S. LISTER, 1986 : *"Dynamic Recrystallization of Minerals"*. In: B. E. Hobbs and H. C. Heard (Ed.), Mineral and Rock Deformation : Laboratory studies. Geophys. Monograph, **36** : 161-199.

J. L. URAI, C. J. SPIERS, C. J. PEACH, R. C. M. W. FRANSEN and J. L. LIEZENBERG, 1987 : *"Deformation Mechanisms Operating in Naturally Deformed Halite Rocks as Deduced from Microstructural Investigations"*. Geol. Mijn. **66** : 165-176.